Committee on Earth Observation Satellites

Working Group on Calibration and Validation

Land Product Validation Subgroup

Global Surface Albedo Product Validation Best Practices Protocol

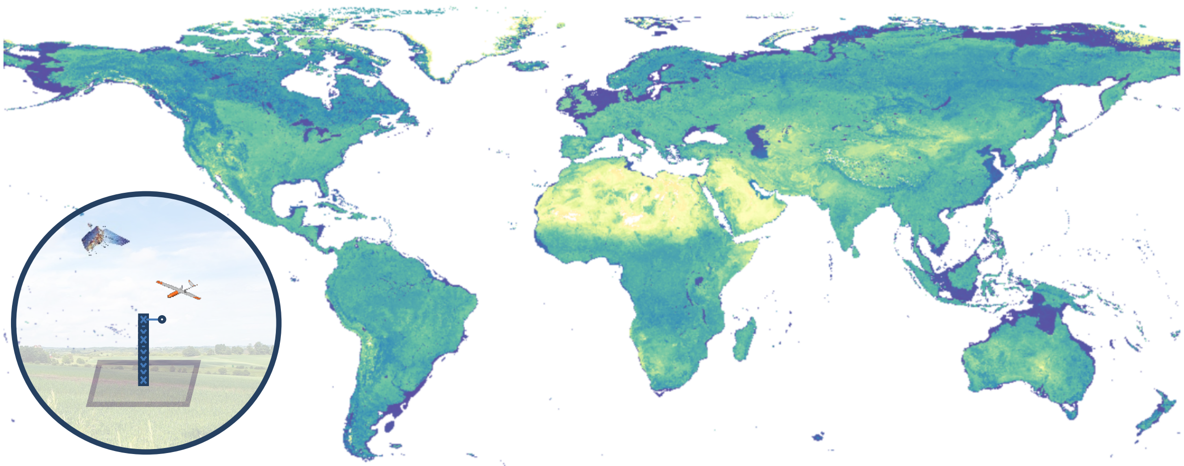

Version 1.0 – 2018

Editors: Zhuosen Wang, Jaime Nickeson, Miguel Román

Authors: Zhuosen Wang, Crystal Schaaf, Alessio Lattanzio, Dominique Carrer, Ian Grant, Miguel Román, Fernando Camacho, Yunyue Yu, Jorge Sánchez-Zapero, Jaime Nickeson

Citation: Wang, Z., Schaaf, C., Lattanzio, A., Carrer, D., Grant, I., Román, M., Camacho, F., Yu, Y., Sánchez-Zapero, J. & Nickeson, J. (2019). Global Surface Albedo Product Validation Best Practices Protocol. Version 1.0. In Z. Wang, J. Nickeson & M. Román (Eds.), Good Practices for Satellite Derived Land Product Validation (p. 45): Land Product Validation Subgroup (WGCV/CEOS), doi: 10.5067/DOC/CEOSWGCV/LPV/ALBEDO.001

List of Revisions

Version	Revision	Date	Author
V0.0	Initial draft outline prepared	September 2015	Román
V1.0	CEOS LPV peer-reviewed version	January 2019	Wang et al.

Editor's Note

This document reflects the views of the surface radiation/albedo product focus area within the CEOS WGCV Land Product Validation sub-group. This focus area provides the community involved in the production and validation of satellite-based albedo products with a forum for documenting accepted best practices in an open and transparent manner, that is scientifically defensible. This Global Surface Albedo Product Validation Best Practices Protocol document (V1.0) has undergone scientific review by remote sensing experts from across the world. It is expected that this best practices protocol document and recommendations will undergo subsequent regular iterations based on community feedback and scientific advancement.

We welcome all interested experts to participate in improving this document and invite the broader community to make use of it for their research and applications related to surface albedo products derived from satellite imagery. All contributors will be recognised as such in the document and on the CEOS WGCV LPV website.

Sincerely,

The Editors,

Zhuosen Wang, University of Maryland, NASA Goddard Space Flight Center
Jaime Nickeson, SSAI, NASA Goddard Space Flight Center
Miguel Román, NASA Goddard Space Flight Center

Chairpersons of the CEOS WGCV Land Product Validation Group

Miguel Román, NASA Goddard Space Flight Center (LPV Chair)
Fernando Camacho, EOLAB (LPV Vice-Chair)

Table of Contents

List of Figures

List of Tables

SUMMARY

The Global Climate Observing System (GCOS) has specified the need to systematically produce and validate surface albedo products. This document provides the recommendations for best practices to be used for the validation of global surface albedo products. Internationally accepted definitions of surface albedo and associated quantities are also provided to ensure thematic compatibility across products and reference datasets. A survey of current validation capacity indicates that progress is being made in terms of spatial representativeness and *in situ* measurement methods, but there continues to be insufficient standardization with respect to performance metrics and the reporting of statistically robust comparisons.

Three albedo validation approaches are identified here: (1) direct point-to-pixel validation, which involves comparisons of satellite products with albedo measured from *in situ*, tower-based instruments, accounting for spatially representativeness; (2) indirect validation, consisting of inter-comparison of various satellite-derived albedo products that vary both temporally and spatially; and (3) upscaling of pixel-to-pixel validation, that relies on high spatial resolution airborne or satellite albedo datasets to assess satellite products at coarser resolution. Finally, the need for an open access facility for performing albedo product validation is identified, as well as a portal for accessing reference albedo datasets.

List of Acronyms and Nomenclature

AERONET	Aerosol Robotic NETwork
AVHRR	Advanced Very High Resolution Radiometer
AWS	Automatic Weather Stations
BHR	Bi-Hemispherical Reflectance
BHRiso	BHR under perfect isotropic illumination conditions
BRDF	Bidirectional Reflectance Distribution Function
BSA	Black Sky Albedo
BSRN	Baseline Surface Radiation Network
CAR	Cloud Absorption Radiometer
CEOS	Committee on Earth Observation Satellites
COP	Conference of the Parties
DHR	Directional-Hemispherical Reflectance
ECV	Essential Climate Variable
EPIFOV	Effective Projected Instantaneous Field of View of Measurement
ESU	Elementary Sampling Unit
EUMETSAT	European Organisation for the Exploitation of Meteorological Satellites
FAPAR	Fraction of Absorbed Photosynthetically Active Radiation
FOV	Field of View
HFOV	Half Field of View
GAW	Global Atmospheric Watch
GBOV	Ground-Based Observations for Validation
GC-NET	Greenland Climate Network
GCOS	Global Climate Observing System
GCM	General Circulation Model
GTOS	Global Terrestrial Observing System
GUM	Guide to the Expression of Uncertainty in Measurement
LBA	Large Scale Biosphere-Atmosphere Experiment in Amazonia
ICS	International Council for Science
IOC	Intergovernmental Oceanographic Commission
ITCZ	Intertropical Convergence Zone
IP	Implementation Plan
LAI	Leaf Area Index
LPV	Land Product Validation
LTER	Long Term Ecological Research
LUT	Look Up Table
MALIBU	Multi AngLe Imaging Bidirectional Reflectance Distribution Function sUAS
MISR	Multi-angle Imaging SpectroRadiometer
MODAPS	MODIS Adaptive Processing System
MODIS	Moderate Resolution Imaging Spectroradiometer

MODTRAN	MODerate resolution atmospheric TRANsmission
MRPV	Modified-Rahman-Pinty-Verstraete
NASA	National Aeronautics and Space Administration
NOAA	National Oceanic and Atmospheric Administration
N2B	Narrowband to Broadband
NECC	Nordic Centre for Studies of Ecosystem Carbon Exchange
NEON	National Ecological Observatory Network
PICS	Pseudo Invariant Calibration Sites
PIFOV	Projected Instantaneous Field of View of Measurement
POLDER	POLarization and Directionality of the Earth's Reflectances
PROMICE	Programme for Monitoring of the Greenland Ice Sheet
RSE	Residual Standard Error
RTLSR	RossThick-LiSparse-Reciprocal
SALVAL	Surface Albedo VALidation tool
SAVS	Surface Albedo Validation Sites Catalogue
SEVIRI	Spinning Enhanced Visible and Infrared Imager
SURFRAD	Surface Radiation Budget Network
STD	Standard Deviation
SZA	Solar Zenith Angle
6SV	Second Simulation of a Satellite Signal in the Solar Spectrum, Vector
TOA	Top of Atmosphere
TOPC	Terrestrial Observation Panel for Climate
UNEP	United Nations Environment Programme
UNESCO	United Nations Educational Scientific and Cultural Organization
UNFCCC	United Nations Framework Convention on Climate Change
USCCC	US-China Carbon Consortium
UV	Ultraviolet
VIIRS	Visible Infrared Imaging Radiometer Suite
WCRP	World Climate Research Programme
WGCV	Working Group on Calibration and Validation
WMO	World Meteorological Organization
WoD	Weight of Determination
WSA	White Sky Albedo

1 INTRODUCTION

This section explains the international framework that has motivated this document, describes surface albedo requirements based on this framework and summaries the goals of the albedo validation protocol.

1.1 Importance of Surface Albedo

Land surface albedo, or the ratio of the radiant flux reflected from the Earth's land surface to the incident flux, is a key forcing parameter controlling the planetary radiative energy budget and the partitioning of radiative energy between the atmosphere and surface. Land surface albedo varies in space and time as a result of both natural processes (e.g. solar illumination, snowfall, and vegetation growth) and human activities (e.g. the clearing and replanting of forests, the sowing and harvesting of crops, the burning and grazing of rangelands) and is a sensitive indicator of environmental vulnerability [*GCOS-92*, 2004]. Consequently, a long-term record of surface albedos for the global landmass is required by climate, biogeochemical, hydrological, and weather forecast models at a range of spatial (from a few metres to 30 km) and temporal (from daily to monthly) scales.

1.2 The UNFCCC and the Global Climate Observing System

The worldwide systematic observation of the climate system is a key requirement for advancing scientific knowledge on the changes that our climate is experiencing. The United Nations Framework Convention on Climate Change (UNFCCC) calls on the Conference of the Parties (COP) to promote and cooperate in this systematic observation of the climate system, including support of existing international programs and networks, as indicated in Articles 4.1(g) and 5 of the Convention. A key dimension for the implementation of those Articles has been the cooperation of the Global Climate Observing System (GCOS), a joint undertaking of the World Meteorological Organization (WMO), the Intergovernmental Oceanographic Commission (IOC) of the United Nations Educational Scientific and Cultural Organization (UNESCO), the United Nations Environment Programme (UNEP) and the International Council for Science (ICS) with its secretariat hosted by the WMO, and whose efforts have been reinforced by decisions taken at various meetings of the COP. The signatories of the UNFCCC have thus adopted the GCOS as the organizing body for climate observations expressed through its Implementation Plans [*GCOS-92*, 2004; *GCOS-138*, 2010]. These Implementation Plans establish the requirements for the systematic monitoring of a suite of Essential Climate Variables (ECV) globally. Albedo is one of the terrestrial ECVs.

1.3 The Role of CEOS WGCV

Surface albedo can be measured *in situ* and indirectly from airborne and spaceborne observations.

While surface albedo is routinely measured at a number of research sites, the measurement network is sparse in many regions of the world and data access is not straightforward as these albedo reference measurements are gathered and distributed by a number of different monitoring networks (the main reference sources are detailed in section §4.1.1 of this document). A baseline albedo dataset should be maintained, and ideally expanded, to become much more representative of the full diversity of global ecosystem conditions.

The process of improving both the space-based observations and the *in situ* networks is embodied in the GCOS Implementation Plans and the accompanying Satellite Supplements [*GCOS-107*, 2006; *GCOS-154*, 2011; *GCOS-200*, 2016]. The Committee on Earth Observation Satellites (CEOS) Working Group on Calibration and Validation (WGCV), and in particular, its subgroup on Land Product Validation (LPV) are designated to play a key coordination role, and to lend the expertise required to validate global surface albedo measurements as identified in GCOS-138:

a. Albedo can be estimated *in situ*, for instance, with opposing pyranometers that integrate the incoming radiation reaching the sensor from an entire hemisphere and that being reflected from the surface. It is routinely measured at a number of research sites dealing with surface climate, ecological, or agricultural issues. CEOS WGCV is playing a coordinating role in supporting these networks. Benchmarking and consistency checks are required for a consistent global archive of surface albedo measurements (p71 of GCOS-154).

b. The development and maintenance of additional reference sites to address the inadequacy in the reference network should be addressed. Efforts building on existing networks (e.g. FLUXNET, SURFRAD, NEON, and BSRN) represent the best possible way to improve this situation (p72 of GCOS-154).

c. The benchmarking and comparison of satellite derived albedo products is essential to resolve differences between products, and to ensure their accuracy and reliability. The CEOS WGCV should lead this activity, in collaboration with GCOS and TOPC, exploiting *in situ* observations from designated reference sites and building on the validation activities currently being undertaken by the space agencies and associated research programs (p74 of GCOS-154).

CEOS considers these roles central to achieving validated global surface albedo products, but at the same time, recognizes the current limitations in both the resources, and in some cases, knowledge within both CEOS and the international expert community. This best practices document includes recommendations (see preamble to this document) from CEOS that should serve to address many of the current limitations.

1.4 GCOS IP Action Items

The role of the CEOS WGCV has been consolidated in to a series of Action Items outlined in the 2010 GCOS Implementation Plan in Support of the UNFCCC (GCOS-138, 2010, aka IP-10) and the 2011 update [*GCOS-154*, 2011], that provides the additional technical details to the Actions and needs in the 2010 plan for several ECVs for which satellite observations make a significant contribution:

In the terrestrial domain, it is essential to obtain global products for most ECVs from a variety of satellite sensors which are supported by *in situ* measurements. A coordinated *in situ* network of terrestrial reference sites must be maintained for (p14 of GCOS-138):

a. Observations of the fullest possible range of terrestrial ECVs and the associated details relevant to their application in model validation;
b. Process studies;
c. Validation of observations derived from Earth observation satellites; and
d. Ways to address intrinsic limitations in some of these.

There are three key requirements for *in situ* measurements at reference sites in the context of long-term global climate measurements listed below:

a. To ensure that a representative set of biomes are properly and consistently documented over long periods of time (decades or more). This will allow the details of land surface changes to be carefully monitored at key locations.
b. To measure key meteorological ECVs to support the interpretation of changes recorded at such sites.
c. To optimize the use of these terrestrial reference sites with essential ground ancillary data for the validation of satellite-derived products.

In responding to the GCOS IP, CEOS has assigned the action items T3, T24 and T25 to the Surface Radiation/Albedo Focus Area of the Land Product Validation Sub-group of its WGCV. This IP outlines the many Actions that will be required to attain a viable observing system to address the needs of the UNFCCC, for albedo, these include:

- *[IP-10 Action T3]* Develop a subset of current LTER and FLUXNET sites into a global terrestrial reference network for monitoring sites; with a sustained funding perspective and co-located measurements of meteorological ECVs; and seek linkage with Actions T4 and T29, as appropriate.

- *[IP-10 Action T4]* Initiate an ecosystem monitoring network acquiring "Essential Ecosystem Records", by exploiting collocation opportunities with the global terrestrial reference network (Action T3) and the network of validation sites (T29)

- *[IP-10 Action T24]* Obtain, archive and make available *in situ* calibration/validation measurements and co-located albedo products from all space agencies generating such products; promote benchmarking activities to assess the quality and reliability of these albedo products.

- *[IP-10 Action T25]* Implement globally coordinated and linked data processing to retrieve land-surface albedo from a range of sensors on a daily and global basis, using both archived and current Earth Observation systems.

1.5 Albedo Requirements

Surface Albedo products are currently used at a range of spatial (from a few meters to 30 km) and temporal (from daily to monthly) scales. Local and regional requirements vary significantly by intended use. However, GCOS has specified a set of global target requirements that in many cases may meet local and regional needs [*GCOS-200,* 2016]:

Spatial resolution: 200/500m horizontal
Temporal resolution: daily
Accuracy: maximum of (5%; 0.0025)
Stability: maximum of (1%; 0.001)

1.6 Rational for Requirements

The objective behind these numbers is to detect the change in radiative forcing equivalent to 20% of the expected total change in radiative forcing per decade due to greenhouse gases and other forcing, i.e. ~0.1 W/m^2 per decade [*Ohring et al.*, 2004]. There are requirements that focus on the temporal stability of a climate data record. Recently, requirements for length of time of a dataset, and the relevance of gaps in the data records have been analyzed [*Loew*, 2014]. While the requirements are global, more accurate and frequent observations over ice and snow would be particularly useful for calculating ice and snow melt. And to study albedo changes over vegetation cover, a time step more than one day is maybe too large to detect a shift of 2/3 days in the growing season during a decade [*Lebourgeois et al.*, 2010; *Planque et al.*, 2017].

Although there are issues with respect to radiometer stability and the implementation of aerosol correction, the specifications of existing (and planned) space-based instruments meet or largely exceed the spatial and temporal sampling requirements of General Circulation Models (GCMs), but a higher frequency of observations would be very useful to guarantee the accuracy and stability of the products, and to support a host of other downstream monitoring applications. Even in the context of climate applications, high spatial resolution products allow studies on the sensitivity of land-surface parameterizations with respect to surface heterogeneity, especially in order to capture snow events and rapid phenologic, hydrologic, and anthropogenic variations.

1.7 Goal of this Document

The goal of this document is to identify the best practices for validating the various (regional and global) satellite surface albedo products. The document will specifically address accuracy assessments with reference surface albedo measurements. The latter should be traceable to *in situ* measurements of known accuracy, and the assessments should be augmented with metrics of precision derived from ensembles of the products themselves. The development of this best practices validation protocol therefore also addresses the GCOS action items described above.

2 DEFINITIONS

This section provides the necessary definitions relevant to global albedo validation.

2.1 Definition of Surface Albedo

Surface albedo is defined as the instantaneous ratio of surface-reflected radiation flux to incident radiation flux over a given spectral interval (dimensionless). Because surface has directional properties, its brightening varies with the angular configuration (illumination and viewing angles). Bi-directional Reflectance Distribution Function (BRDF) describes these directional properties of the surface reflectance according to all angular configurations. Inherent albedo is the directional-hemispherical surface reflectance integrated from surface BRDF over all viewing angles and independent of the atmospheric conditions. The actual surface albedo depends on both the anisotropy of the surface reflective properties and the scattering process in the atmosphere [*Liang et al.*, 1999]. Reflectance from land surface is spectrally coupled with aerosol scattering. They can be imagined as two layers having strong spectral interaction (see for instance Pinty et al., 2000). In particular over bright surface it is a challenging task to distinguish between the contribution due to surface reflectance and aerosol scattering and multiple scattering between the two layers from remote sensing measurements. Albedo can be defined for broad spectral domains or for spectral bands of finite width. This definition was adopted across the various international groups (CEOS WGCV, GTOS, WMO, GCOS).

2.2 Definitions of Albedo Retrieval Associated Parameters

Albedo is a physical parameter included in the list of Essential Climate Variables (ECV). While direct ground albedo measurements at the surface are possible, this is not the case for instruments on board satellites. A number of albedo quantities have therefore been introduced in particular for measurements acquired from space [*Pinty et al.*, 2005; *Schaepman-Strub et al.*, 2006].

2.2.1 Black-Sky Albedo (BSA)

Black-sky albedo or Directional Hemispherical Reflectance (DHR) is the albedo in the absence of any diffuse irradiance component (no atmospheric scattering), with only a direct illumination component. GCOS (2004a) specified black-sky albedo as the product required for climate change purposes. Since the DHR is a function of the Solar Zenith Angle (SZA); it is computed for a specific time (usually local solar noon) or a default value of the SZA.

$$\mathrm{BSA}(\theta_i) = \rho(\theta_i, \varphi_i, 2\pi) = \frac{d\Phi_r(\theta_i,\varphi_i,2\pi)}{d\Phi_i(\theta_i,\varphi_i)} = \frac{\mathrm{dA} \int\int \mathrm{dL}_r(\theta_i,\varphi_i;\theta_r,\varphi_r)\cos\theta_r\sin\theta_r d\theta_r d\varphi_r}{d\Phi_i(\theta_i,\varphi_i)}$$
$$\frac{d\Phi_i(\theta_i,\varphi_i) \int\int f_r(\theta_i,\varphi_i;\theta_r,\varphi_r;\lambda)\cos\theta_r\sin\theta_r d\theta_r d\varphi_r}{d\Phi_i(\theta_i,\varphi_i)} \quad (1)$$
$$\int\int f_r(\theta_i,\varphi_i;\theta_r,\varphi_r;\lambda)\cos\theta_r\sin\theta_r d\theta_r d\varphi_r \,.$$

Where ρ is reflectance or albedo, Φ is radiant flux, $\theta$is zenith angle, $\varphi$is azimuth angle, *i* is incident*, r* is reflected*,* λ is wavelength [*Schaepman-Strub et al.*, 2006].

2.2.2 White-Sky Albedo (WSA)

White-sky albedo or bi-hemispherical albedo under isotropic illumination ($\mathrm{BHR_{iso}}$) is the albedo in the absence of any direct illumination component but only comprised of isotropic diffuse illumination. This component is sensitive to the intrinsic coupling between the surface and the scattering atmosphere.

$$\mathrm{WSA} = \rho(2\pi; 2\pi) = \frac{1}{\pi}\int\int \rho(\theta_i, \varphi; 2\pi)\cos\theta_i\sin\theta_i d\theta_i d\varphi_i \quad (2)$$

Where ρ is reflectance or albedo, Φ is radiant flux, $\theta$is zenith angle, $\varphi$is azimuth angle, *i* is incident [*Schaepman-Strub et al.*, 2006].

2.2.3 Blue-Sky Albedo

Blue-sky albedo comprises both direct and diffuse components and represents the albedo of the surface with respect to specific atmospheric conditions. For snow-free surfaces, a simple form of blue sky albedo can be calculated with an assumption of isotopically diffuse radiation and can be expressed as a linear combination of DHR and BHRiso [*Lewis and Barnsley*, 1994; *Lucht et al.*, 2000; *Pinty et al.*, 2005]:

$$BlueSkyAlbedo = \big(1 - skyl(\theta_i)\big)BSA(\theta_i) + skyl(\theta_i)WSA \quad (3)$$

Where *skyl*(θ_i) is the proportion of diffuse irradiation at a certain SZA θ_i. The proportion of diffuse radiation comes from the scattering of light and the reflection and transmission from clouds and aerosols in a blue sky.

However, the effects of multiple scattering and anisotropic diffuse illumination should be considered more carefully for fully snow-covered areas due to the very high reflectance of snow and large solar zenith angles of high latitudes. Therefore, the full expression the blue-sky albedo should be used for snow-covered areas [*Román et al.*, 2010].

2.2.4 Surface Anisotropy

Natural surfaces reflect light in different ways and different amounts according to the viewing and illumination conditions and the reflective character of the surface. Thus, such behaviour depends on the level of anisotropy of the surface itself. Surface anisotropy is quantitatively described by with the so-called BRDF [*Schaepman-Strub et al.*, 2006].

2.3 Definition of Spatial and Geometrical Aspects

The following definitions were adapted from the Global Leaf Area Index Product Validation Good Practices document [*Fernandes et al.*, 2014].

2.3.1 Elementary Sampling Unit (ESU)

An Elementary Sampling Unit (ESU) is a contiguous spatial region over which the surface albedo can be measured through *in situ* measurement. The ESU corresponds to the finest spatial scale of surface albedo estimates used for reference. The ESU size is the footprint of *in situ* pyranometer measurements which are based on the instrument height (Figure 1).

$$f = 2 \cdot H \cdot \tan\,(HFOV) \tag{4}$$

where f is the circular footprint of ground tower measurements, H [m] is the tower height, and $HFOV$ [degrees] is its half field of view. Generally, HFOV equalling 81° is used for *in situ* albedo measurements [*Michalsky et al.*, 1995].

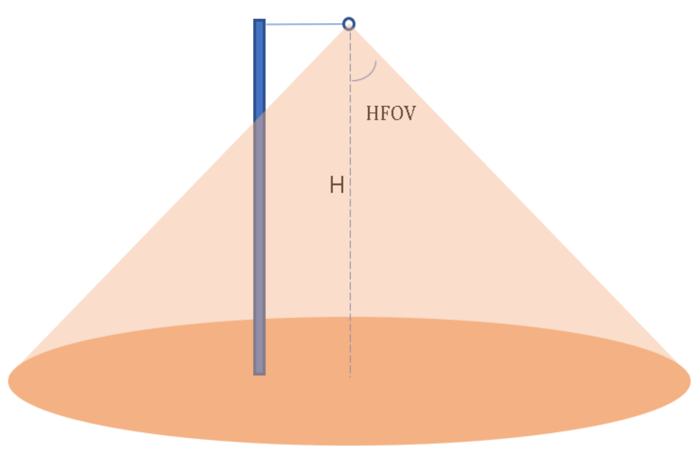

Figure 1. The footprint of *in situ* pyranometer measurements.

2.3.2 Local Horizontal Datum

The local horizontal datum is the plane containing the tangent to the local geoid corresponding to the centre of an ESU or mapping unit. For sloped terrain corrections to surface albedo estimates, the increased surface area of the slope may need to be incorporated, depending on the survey method.

2.3.3. Projected Instantaneous Field of View of Measurement (PIFOV)

The ground projected instantaneous field of view (PIFOV) is the area on the ground corresponding to the region over which a measurement is obtained. For radiometric measurements, this area is defined as the region where the instrument point spread function, including all processing aspects, except for spatial resampling, exceeds a specified threshold. The majority of imaging scanners, including satellite imagers, have a PIFOV on flat ground on the order of twice the inter-pixel sampling distance. The PIFOV of an *in situ* instrument will vary with the height and angular sampling of the instrument.

2.3.4 Satellite Measurement Geolocation Uncertainty

Geolocation uncertainty, for surface albedo validation, corresponds to the planimetric uncertainty of a satellite measurement located on the same projection and datum as the reference ESU (or study site) surface albedo estimate. Geolocation uncertainty is often reported in nominal terms and is based on a normal distribution of errors. Acquisition specific biases are often possible, so the geolocation uncertainty should also be visually assessed in comparison to reference vector layers whenever possible.

2.3.5 Mapping Unit

A mapping unit is the spatial region on the Earth's surface corresponding to a product value for a specified temporal extent. Satellite based surface albedo products represent gridded digital layers in a specified map projection rather than per nominal PIFOV location. As such, these products include a spatial generalization corresponding to the transformation of the surface albedo estimate over each PIFOV to the surface albedo estimate in the mapping grid unit. Considering that GCOS requires gridded surface albedo products at a constant spatial resolution, the CEOS Surface Albedo validation protocol assumes that the uncertainties due to this generalization or due to temporal aggregation are part of the total product uncertainty.

2.4 Definition of Validation Metrics

Albedo validation is the process of assessing the quality of satellite albedo products using independent reference datasets. Definitions of validation metrics applicable to surface albedo validation drawn from experimental statistics reported below are mainly from the Joint Committee for Guides in Metrology (JCGM) guide to the expression of uncertainty in measurement, referred to as GUM-2008[*GUM-2008*, 2008] and from GCOS-154:

- **Error** (of measurement) is "the result of a measurement minus a true value of the measurand". The true value (of a quantity) is the "value consistent with the definition of a given particular quantity". Since a true value cannot be usually determined, in practice a conventional true value is used. The conventional true value (of a quantity) is the "value attributed to a particular quantity and accepted, sometimes by convention, as having an uncertainty appropriate for a given purpose". Traditionally, an error is viewed as having two components, namely, a random component and a systematic component. The random error is the "result of a measurement minus the mean that would result from an infinite number of measurements of the same measurand carried out under repeatability conditions" and the systematic error is the "mean that would result from an infinite number of measurements of the same measurand carried out under repeatability conditions minus a true value of the measurand".

- **Uncertainty** is a "parameter, associated with the result of a measurement, that characterizes the dispersion of the values that could reasonably be attributed to the measurand". Uncertainty includes bias and precision errors and can be estimated by the Root Mean Square Error (RMSE).

- **Accuracy** is the degree of "closeness of the agreement between the result of a measurement and a true value of the measurand". Commonly, accuracy is represented as a description of systematic errors and a measure of statistical bias. **Bias** is the systematic error between albedo products and their reference estimates, i.e. it describes the average deviation from the reference, which is given by the average difference between the albedo product and its reference estimate.

- **Precision or repeatability** (of results of measurements) is the "closeness of the agreement between the results of successive measurements of the same measurand carried out under the same conditions of measurement". Commonly, precision represents the dispersion of product retrievals around their expected value and can be estimated by the standard deviation (STD) of the difference between retrieved albedo and the corresponding reference estimates.

-**Stability** is the extent to which the error of a product remains constant over a long period, typically a decade or more. The relevant component of error of a product for climate application is often the systematic component defined by the mean error over a period such as a month or year. Values quoted under the heading "stability" in this document refer to the maximum acceptable change in systematic error per decade, except for variables for which trends are usually expressed in terms of an annual rate of change, in which case the stability is expressed in terms of this rate of change. Stability of the random component may also be a requirement however, in particular for monitoring long-term changes in extremes.

- **Completeness** is the proportion of valid retrievals over an observation domain at any given time, that over time indicates its frequency and continuity.

It should be noted that strong and/or multiple outliers affect the classical metrics described above (i.e. mean and STD): in such cases using the median in lieu of the mean to estimate systematic error and the median absolute deviation as a measure of precision is more suitable and should be included in the validation effort.

3 GENERAL CONSIDERATIONS FOR SATELLITE SURFACE ALBEDO PRODUCTS

3.1 The current global satellite albedo products

The current global satellite albedo products are listed on the CEOS LPV subgroup website (https://lpvs.gsfc.nasa.gov/producers2.php?topic=SurfRad). Most of the satellite albedo products are generated based on models that consider surface anisotropy and are mainly derived from semi-empirical linear kernel driven models such as RossThick-LiSparse-Reciprocal (RTLSR) and variations; the Rahman-Pinty-Verstraete (RPV) model, and the direct estimate method.

3.1.1 Semi-empirical approach

The semi-empirical linear kernel driven BRDF model consists of isotropic, volumetric and geometric scattering [*Ross, 1981; Li and Strahler, 1986; Li and Strahler, 1992; Roujean et al., 1992; Wanner et al., 1995*] to describe the reflectance anisotropy. The isotropic parameter represents the surface reflectance illuminated and viewed at nadir, and is mainly a function of the optical properties of vegetation and soil reflectance. The volumetric and geometric-optical parameters describe the radiative transfer type volume-scattering and shadowed surface-scattering effects, and are therefore related to the anisotropic pattern of the land surface. The RossThick model is used for the volumetric kernel in the RTLSR model and the LiSparse model is selected for the geometric kernel.

$$R(\theta, v, \phi, \lambda) = f_{iso}(\lambda) + f_{vol}(\lambda)k_{vol}(\theta, v, \phi) + f_{geo}(\lambda)k_{geo}(\theta, v, \phi) \quad (5)$$

where θ, υ and ϕ are solar zenith, view zenith and relative azimuth angles; k_{geo} and k_{vol} are the volumetric and geometric kernels; and f_{iso}, f_{geo} and f_{vol} are the isotropic, geometric and volumetric weights given to the model parameters. $R(\theta, v, \phi, \lambda)$ is the modelled reflectance at given geometry (θ, v, ϕ) of band λ.

In the RPV model [Rahman et al. 1993], the surface is described as an amplitude component and an angular function accounting for the anisotropy:

$$R_{sfc}(\Omega, \Omega_0; R_0, R_c, b, k) = R_0 \check{R}_{sfc}(\Omega, \Omega_0; R_c, b, k) \quad (6)$$

R_{sfc} represents the angular surface reflectance. The angular shape (bowl or bell) of the BRF fields is controlled by parameter *k* [*Pinty et al.*, 2002], the parameter *b* establishes the degree of forward versus backward scattering and the hot spot effect is described by parameter R_c. The view direction Ω is characterized by the view zenith and azimuth angles, and Ω_0 represents the direction of the Sun. $\check{R}_{sfc}$is the angular function (itself implemented as the product of three functions) [*Pinty et al. 2000a, Pinty et al. 2000b*, *Taberner et al.*, 2010]. The gaseous absorption is corrected, while the surface contribution and the aerosol optical depth are jointly retrieved, trying to account for the natural coupling between the surface and the scattering atmosphere (see Section 2.1).

The WSA and BSA are calculated using the equations in Section 2.2. The surface energy balance studies require broadband shortwave albedo (0.25–5.0μm) in land surface models [*Roesch and Roeckner*, 2006; *Wang et al.*, 2016]. Satellite data are usually provided as multiple bands with narrow spectral ranges. Narrow-to-broadband conversion coefficients are used to produce shortwave broadband albedo [*Liang*, 1999, 2001; *Stroeve et al.*, 2005; *Shuai et al.*, 2014; *Liu et al.*, 2017].

3.1.2 The Direct Estimate method

The direct estimate method directly links the surface albedo to the Top of Atmosphere (TOA) reflectance observed by satellite sensors without a separate atmospheric correction procedure, through the use of a Look Up Table (LUT) and a linear regression equation [*Wang et al.*, 2013]:

$$a = f(\rho_1, \rho_2, \dots, \rho_n) \tag{7}$$

Where a is surface broadband shortwave albedo, ρ_n is narrowband TOA reflectance for band *n,* and *f* represents a linear regression equation.

The training data used to establish the linear regression equation are obtained through radiative transfer model simulations (e.g. Second Simulation of a Satellite Signal in the Solar Spectrum, Vector (6SV), MODerate resolution atmospheric TRANsmission (MODTRAN)) incorporating atmospheric conditions and a surface BRDF database (e.g. the MODIS or POLarization and Directionality of the Earth's Reflectances (POLDER) BRDF products). The regression coefficients vary with satellite solar-view geometry, as well as aerosol type and surface type, and are stored in the LUT.

3.2 Geometric Considerations

Surface albedo products are based on satellite measurements whose effective projected instantaneous field of view (EPIFOV) will not exactly match the mapping unit for several reasons:

- The pixel size changes with the across-track scan angles. Generally, the pixel size on the ground increases with distance from the nadir point for wide swath whisk broom systems.

- Terrain effects change the shape, nominal location and, to a lesser extent, size of the ground projected instantaneous field of view (PIFOV). Certain processing chains (such as the MODIS adaptive processing system [MODAPS]) apply orthorectification to provide a precise nominal location for all terrain. However, the majority of sensor processing chains do not include orthorectification by default. It should be noted that no current processing chain accounts for the variable shape of the PIFOV.
- Most surface albedo products are derived from reflectance measurements resampled to a final projection system and geoid and are gridded to pixels with a specific spatial resolution based on footprint coverage and data quality. The resampling and gridding processes tends to reduce information at high spatial frequencies. These effects should be included in the error analysis.
- Several albedo products are retrieved from multi-angular observations to establish the surface reflectance anisotropy. The footprint of these multi-angular observations will be different. Therefore, the effective spatial resolution of the albedo products usually represents a somewhat larger surface area than the pixel grid size and should be considered in the use of albedo products [*Campagnolo et al.*, 2016].

3.3 Uncertainty related to albedo products

The uncertainty of remote sensing measurements has contributions from terms that account for several processes used in the conversion of raw measurements to the input needed for the retrieval of the surface albedo. The majority of satellite derived albedo products rely on atmospherically corrected angular surface reflectance as model input. The uncertainty of sensor calibration, and of atmospheric correction related to surface reflectance should be quantified. The broadband albedo is derived from narrowband albedo values through the use of narrowband-to-broadband (N2B) conversion coefficients. The uncertainty related to this N2B conversion and the albedo retrieval model should also be considered.

3.3.1 Uncertainty related to the sensor calibration

The original sensor measurements are quantified as voltage or digital counts. Sensor calibration establishes the conversion from digital counts (voltage) to radiances. The calibration coefficients can be derived by comparing the sensor signal with an absolute standard reference prior to launch. However, sensors degrade with time on orbit due to thermal, mechanical and electrical effects, or exposure to ultraviolet radiation etc [*Müller*, 2014]. Post-launch calibration is necessary to ensure the quality of the derived variables and products. The calibration and uncertainty can be quantified by using a solar diffuser view, a moon view, and pseudo invariant calibration sites (PICS) etc. [*Toller et al.*, 2013; *Lyapustin et al.*, 2014; *Mishra et al.*, 2014].

3.3.2 Uncertainty related to atmospheric corrections

The atmospheric correction is usually performed through a radiative transfer model with atmospheric parameters (e.g. aerosol, water vapour, etc.) to derive the surface reflectance. The uncertainty of the radiative transfer model and the accuracy of the atmospheric parameters should be quantified to fully evaluate the uncertainty of the resultant surface reflectance.

3.3.3 Uncertainty related to narrow-to-broadband conversions

Narrow-to-broadband conversion algorithms have reported uncertainties of 5–10% [*Liang*, 2001; *Govaerts et al.*, 2006]. The average residual standard error (RSE) is about 0.02 for most sensors for the three broadband albedos (total-shortwave, -visible, and - near-IR) [*Liang et al.*, 2003]. Furthermore, algorithms usually use external snow mask information and select only the observations that are snowy or snow-free for the composite period of the albedo product. Snowy and snow-free observations are not mixed together by semi-empirical BRDF approaches (which can use different kernel functions in the case of snow). False snow detection could introduce uncertainty in the BRDF inversion, and the narrow-to-broadband conversion usually uses different set of coefficients for the case of snow (or ice).

3.3.4 Uncertainty related to albedo retrieval algorithms

Albedo retrieval algorithms usually cannot exactly simulate the all kinds of realistic surface conditions. The limitation of the albedo retrieval models should be analyzed. The accuracy of albedo models may decrease with an increase of zenith angles. The Weight of Determination (WoD) is used to describe, for a linear kernel model, the albedo uncertainty relative to the uncertainty of the input reflectances due to the limitations in angular sampling [*Lucht and Lewis*, 2000; *Shuai et al.*, 2008]. The covariance matrix is reported to describe the Spinning Enhanced Visible and Infrared Imager (SEVIRI) albedo retrieval uncertainty [*Geiger et al.*, 2008]. The retrieval error was analyzed for the albedo estimated from the European Meteosat first generation satellites [*Govaerts and Lattanzio*, 2007]. The uncertainty of albedo retrieval algorithms can also be evaluated by comparing the algorithms simulated directional reflectance values with directional reflectances actually observed.

3.3.4 Uncertainty related to missed cloud screening

Any land retrieval should first attempt a robust and reliable cloud screening. The effect of not removing clouds has a twofold effect. It hampers the quality of each single retrieval but it also introduces a spurious albedo pattern depending on the location and the season. For instance, not removing clouds in the tropical regions of the African continent will generate an artificial increase in albedo in the months of June-July-August (north of the Equator) or January-February-March (south of the Equator) due to the shift of the Intertropical Convergence Zone (ITCZ) and its impact on the African Monsoon regime. Clouds should therefore be masked before retrieval, but it might be necessary to remove the remaining cloud contamination as post-processing, even with the potential danger of erasing good measurements [*Lattanzio et al. 2015*]. From the point of view of climate studies and applications it is better to have fewer but more reliable retrievals. A discussion of the impact on surface albedo retrieval with Meteosat First Generation imagery due to residual clouds that had not been corrected screen out can be found in [*Fell et al. 2012*]. The corresponding uncertainty can be up to 100%, much higher than the average retrieval uncertainty of ~10-20% in tropical regions.

4 GENERAL CONSIDERATIONS FOR ALBEDO REFERENCES

4.1 Reference surface albedo estimates

Reference surface albedo values are required to evaluate the accuracy and to a lesser extent the spatial and temporal precision of surface albedo products. The reference albedo datasets can be derived as the ratio of reflected irradiance to the surface received irradiance. This section surveys ground networks that provide measurements of surface albedo and identifies good practices related to the production of reference surface albedo estimates.

4.1.1 Existing *in situ* tower-based albedo references

In situ tower-based albedo reference measurements are acquired from upwelling and downwelling flux measured by paired pyranometer installed on flux towers. The measurement of surface albedo should closely follow the guidelines used by the Baseline Surface Radiation Network (BSRN) [*Ohmura et al.*, 1998; *McArthur*, 2005] to provide continuous, consistent, long term measurements of the surface radiation fluxes adhering to the highest achievable standards of measurement archiving and uncertainty. These standards [*McArthur*, 2005; *GCOS-107*, 2006] require that radiation variables be reported as one-minute values of mean, minimum, maximum and standard deviation with target uncertainties of less than 5 percent or 10 W m^{-2}.

Several networks with *in situ* tower-based albedo measurements are commonly used to validate currently available operational albedo products (e.g. SURFRAD, NEON, BSRN). These existing observational networks (Table 1) include appropriate tower sites with the necessary infrastructure (e.g. human maintenance, radiation instrument availability, site accessibility, and power needs) to measure radiation variables for albedo calculations. The challenge for these networks is in the use of best practices in measurement, calibration and archive protocols as adhered to by the BSRN, and to provide timely access [*Baret et al.*, 2005] to the data. In addition to radiation measurements, the atmospheric state measurements vital to correlate surface and satellite-based quantities are also collected at many of these sites as part of regional or global meteorological or atmospheric networks contributing to the WMO Global Atmospheric Watch (such as the Aerosol Robotic NETwork - AERONET).

While the extent of these surface measurements is currently insufficient to systematically validate remote sensing products in a global sense, they do complement a range of scientific efforts aimed at comparing and benchmarking the various albedo products currently being generated. Pursuing these networking activities will be essential to ensure the quality and reliability of future albedo products, and a step toward more accurate and consistent albedo reference information for the global landmass and the development of associated standards.

Reference sites for surface albedo validation must fulfill the following requirements:

- Spatial representative of an albedo product pixel, thus the scale of spatial heterogeneity must not be greater than the minimum mapping unit of the product under validation
- Representative of different surface types
- Stable over time to allow characterization of temporal stability

Ideal *in situ* albedo measurements need to be continuous in time with a temporal sampling rate of less than 30 minutes. If the satellite albedo products are derived at overpass time or at local solar noon, the time difference between *in situ* albedo measurements and satellite overpass time or local solar noon could lead to large biases in validation. Figure 2 shows the location of the sites from the reference networks with publicly available albedo measurements. The spatial representativeness of several sites has been analysed for the validation of coarse spatial resolution albedo products [*Román et al.*, 2009; *Cescatti et al.*, 2012; *Wang et al.*, 2012, 2014].

Copernicus Global Land Monitoring Service partners developed a centralised validation database, the Ground-Based Observations for Validation of Copernicus Global Land Products (GBOV, http://gbov.copernicus.acri.fr), that offers direct access to a set of reference measurements. Currently the GBOV dataset has 20 sites with albedo reference data available.

Table 1. *In situ* tower-based albedo reference networks.

Networks	**Reference / Remark**
BSRN	https://bsrn.awi.de/
BSRN-SURFRAD	https://www.esrl.noaa.gov/gmd/grad/surfrad/
FLUXNET	http://fluxnet.fluxdata.org/
NEON	http://www.neonscience.org/
GC-Net	http://cires1.colorado.edu/steffen/gcnet/
PROMICE	https://www.promice.dk/home.html

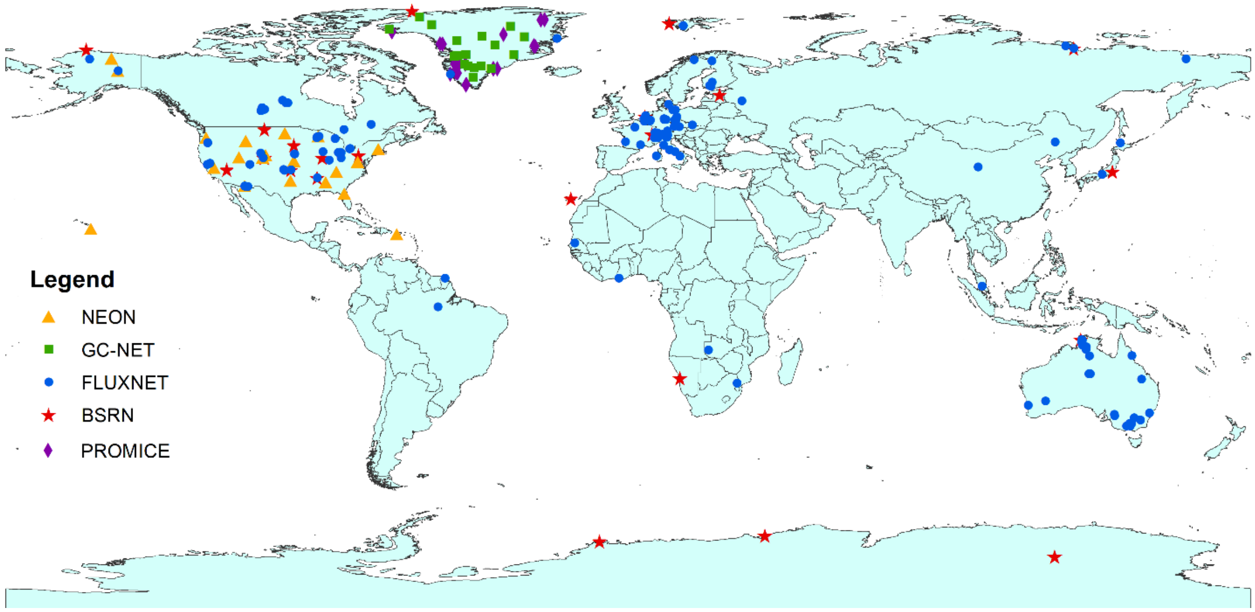

Figure 2.The location of *in situ* tower-based albedo reference sites. The latitude/longitude of each site is listed in Appendix A.

4.1.1.1 The Baseline Surface Radiation network (BSRN)

The World Climate Research Programme (WCRP) Radiative Fluxes Working Group initiated the BSRN to support the research projects of the WCRP and other scientific programs that aim at detecting important changes in the Earth's radiation field at the surface. BSRN is now recognized as the GCOS baseline network for surface radiation [*GCOS-92*, 2004]. While these spatially-limited BSRN (Figure 1) tower sites provide the highest-quality measurements available of radiation at the surface, the network needs to be expanded and adequately supported to achieve a more representative global coverage [*GCOS-92*, 2004]. While all BSRN sites measure downwelling irradiance, not all measure the upwelling radiance required to measure albedo.

The primary objective of the Surface Radiation Budget Network (SURFRAD) [*Augustine et al.*, 2000], established in 1993, is to support climate research with accurate, continuous, long-term measurements of the surface radiation budget over the United States by the National Oceanic and Atmospheric Administration (NOAA) as part of the BSRN [*Ohmura et al.*, 1998]. Seven SURFRAD sites are operating in climatologically diverse regions in the US. Quality-controlled measurements of upwelling and downwelling shortwave radiation, direct and diffuse fraction, and meteorological parameters are provided once per minute. The SURFRAD instruments are meticulously maintained, and all instruments are replaced on an annual basis with freshly calibrated instruments.

4.1.1.2 FLUXNET

FLUXNET was started to provide ground truth support for the new Earth Observing System (EOS) and then received enough support from the scientific community to develop regional networks such as EuroFlux, AmeriFlux and AsiaFlux, among others. The role of FLUXNET is to unite regional networks to form a global network and to provide a data portal and database. FLUXNET [*Baldocchi et al.*, 2001] provides continuous observations of ecosystem level exchanges of CO2, water and energy, and micrometeorological parameters at diurnal, seasonal, and interannual time scales. More than 900 sites worldwide have been registered as members of the FLUXNET (e.g. CarboEurope IP, AmeriFlux, LBA, AsiaFlux, ChinaFlux, USCCC, Ozflux, CarboAfrica, KoFlux, NECC, and AfriFlux, see also http://fluxnet.fluxdata.org/about/regional-networks/).

4.1.1.3 The National Earth Observatory Network (NEON)

NEON consists of 47 terrestrial tower sites located across 20 eco-climatic domains in the US with one "core site" within each domain. Each of the 20 core terrestrial sites represents a different ecosystem region with varying vegetation types and climates [*Hamilton et al.*, 2007; *Schimel et al.*, 2007; *Kampe*, 2010]. The land cover types of the NEON sites include forest, grassland, tundra and shrub. Long-term (30 year) data acquisition from NEON will provide site-based field ecological and climatic observations which can be coupled with regional and national-scale airborne remote sensing observations to describe land use and climate-driven seasonal change. Kipp & Zonen CMP22 pyranometers are used for the shortwave radiation measurements. Ventilation and heater controls are recommended to prevent dew, frost, rime ice, and snow forming or accumulating on the sensors, that would result in inaccurate data. NEON provides Kipp and Zonen CVF 3 ventilation unit for ventilation and heating of each of their pyranometer. Wang et al. (2017) analysed the spatial representativeness of these sites for the validation of coarse spatial resolution albedo products (e.g. MODIS, Visible Infrared Imaging Radiometer Suite (VIIRS)).

4.1.1.4 GC-Net

The Greenland Climate Network (GC-Net) Automatic Weather Stations (AWS) (http://cires1.colorado.edu/science/groups/steffen/gcnet/), established in the 1990s, are distributed widely across the Greenland ice sheet [*Steffen and Box*, 2001]. The shortwave fluxes are measured by pairs of LICOR 200SZ photoelectric diode pyranometers. The pyranometers are horizontally levelled to measure incident and reflected hemispheric radiant flux density (irradiance), and to provide hourly average shortwave albedo data from 15-second samples. Steel cables have been attached to stabilize GC-Net towers from strong winds. The LI-COR 200SZ is relatively small in size and mass, allowing the sensor body to adjust more rapidly to temperature changes than larger radiometers needed for the ice sheet environment. The detector surface is horizontal, with no dome to avoid frost accretion. The spectral sensitivity of the LI-COR instrument, under a standard atmosphere, gauges downward shortwave irradiance over the ice sheet within the 5% error specification. However, the Li-COR 200SZ only measures the downward and upward solar energy in a restricted spectral range (0.4–1.1μm). Thus, a correction is needed to use these data for broadband shortwave albedo (0.3-5μm) validation. The AWS-reflected irradiance data are corrected for any spectrally sensitive biases based on results from comparisons with more accurate pyranometers at regularly maintained AWS locations (Eppley PSP measurements at Swiss Camp and TUNU-N; with Kipp and Zonen CM21 measurements at Summit). The accuracy of the daily *in situ* albedo observations after correction is estimated to be 0.035 [*Stroeve et al.*, 2006].

4.1.1.5 Programme for Monitoring of the Greenland Ice Sheet (PROMICE)

In-*situ* tower-based albedo measurements over ice and snow are particularly useful for assessing the product performance in a global range. The PROMICE was initiated in 2007 with the aim of gaining an insight into the causes of the ice-mass budget changes based on quantitative observations. PROMICE automatic weather station data over Greenland provides albedo measurements in the ablation area of the ice sheet, while GC-Net sites are located primarily in the accumulation area. The albedo of PROMICE sites are measured using Kipp and Zonen CNR1 or CNR4 net radiometer.

4.1.2 High spatial resolution airborne/spaceborne albedo references

The footprint of *in situ* surface albedo reference site needs to represent the entire satellite pixel size for accurate albedo validation. The validation would be biased if the footprints of the *in situ* albedo measurements are significantly larger than the albedo product pixel size over a heterogeneous surface. In these cases, high spatial resolution airborne/spaceborne albedo references are more appropriate for the validation exercise. The high spatial resolution airborne/spaceborne albedo should first be evaluated using *in situ* albedo reference data. Coarse spatial resolution albedo products can then be evaluated by comparing with the albedo estimates from aggregations of the high spatial resolution albedo values.

National Aeronautics and Space Administration's (NASA's) airborne Cloud Absorption Radiometer (CAR) provides thousands of multi-angular surface observations per flight which can be used to retrieve high resolution (30m) surface albedo using a BRDF/albedo model. The retrieved albedo has been evaluated with *in situ* albedo measurements with a high accuracy [*Román et al.*, 2011, 2013]. High spatial resolution albedo can also be measured by downward-facing pyranometer mounted on UAV paired with upward-facing pyranometer from fixed pole [*Levy et al.,* 2018]. In addition, Landsat (30 m) and Sentinel-2 (20 m) surface albedo have been generated and validated [*Shuai et al.*, 2011; *Li et al.*, 2018]. The surface anisotropy BRDF values from the MODIS albedo products are used to convert the near-nadir Landsat observations to hemispherical surface albedo. Landsat 30 m snow-free shortwave albedo from all seasons have been shown to achieve nearly absolute accuracy of ±0.02– 0.05 in comparison with *in situ* tower-based albedo measurements from SURFRAD sites.

4.2 Elementary Sampling Unit (ESU) Mapping Unit

Most best practices for surface albedo validation require an estimate of the spatial mapping unit corresponding to each sampled ESU. The ESU mapping unit should correspond to the area over which the surface albedo together with its associated measurement error are representative. The ESU should also be large enough to be either directly co-located with the surface albedo product mapping units or with ancillary information than can be used to upscale multiple ESUs over a region. These considerations often drive the specification of the ESU.

According to results obtained for NASA's MODIS and VIIRS [*Wang et al.*, 2012, 2014; *Liu et al.*, 2017], the *in situ* tower-based surface albedo validation needs to be performed over spatially uniform or relatively homogeneous sites. High-resolution surface reflectance and albedo datasets can be used to assess the spatial representativeness of *in situ* albedo measurements and to select appropriate validation sites. Román et al. (2009) proposed a semi-variogram method to estimate the spatial variability of surface albedo around stations of interest, and to evaluate the spatial representativeness of in-situ measurements based on the footprint of the tower albedometer. The validation of coarse spatial resolution surface albedo products over heterogeneous areas therefore requires the use of high spatial resolution albedo estimates from *in-situ* albedo measurements nested with airborne and spaceborne measurements.

4.3 Uncertainty related to albedo references

The performance of a validation exercise is strongly dependent on the uncertainty of the reference surface albedo datasets. Reference surface albedo uncertainties should be meticulously reported, including uncertainties associated with the upscaling or with the geometric models used, and to some extent, the uncertainty associated with the representativeness of the ESU.

4.3.1 Uncertainties related to *in situ* albedo references

The uncertainty of *in situ* tower-based albedo measurements depends on the absolute accuracy of the pyranometers and the associated non-ideal cosine response. Most of the errors associated with the absolute accuracy of the instrument are similar for the upward and downward fluxes and therefore compensate. Overall the expected accuracy is in the order of 4–7% in clear sky and 1–4% in overcast conditions [*Pirazzini*, 2004; *Pirazzini et al.*, 2006; *Cescatti et al.*, 2012]. The uncertainty could be greater if the pyranometer is not properly ventilated and heated to prevent the effects of frost, snow/ice.

4.3.2 Uncertainties related to high spatial resolution albedo estimates

High spatial resolution airborne or spaceborne albedo estimates are usually retrieved from multi-angular observations (e.g. MALIBU, https://viirsland.gsfc.nasa.gov/Campaigns.html) or nadir estimates (e.g. Landsat, Sentinel-2) [*Shuai et al.*, 2011] based on albedo models. Therefore, the uncertainty related to the optical sensors and the albedo models (section 3.3) should be considered.

5. GENERAL STRATEGY FOR THE VALIDATION OF SURFACE ALBEDO PRODUCTS

5.1 CEOS Validation Stages

The CEOS WGCV Land Product Validation (LPV) sub-group has identified four validation levels corresponding to increasing spatial and temporal representativeness of samples used to perform direct validation (Table 2) (https://lpvs.gsfc.nasa.gov/). The surface albedo validation protocol includes these aspects and supplements them with requirements for assessing the spatial and temporal precision of individual products.

Table 2. The CEOS WGCV Land Product Validation Hierarchy

Stage 0	No validation. Product accuracy has not been assessed. Product considered beta.
Stage 1	Product accuracy is assessed from a small (typically < 30) set of locations and time periods by comparison with *in situ* or other suitable reference data.
Stage 2	Product accuracy is estimated over a significant set of locations and time periods by comparison with reference *in situ* or other suitable reference data. The spatial and temporal consistency of the product and with similar products has been evaluated over globally representative locations and time periods. Results are published in the peer-reviewed literature.
Stage 3	Uncertainties in the product and its associated structure are well quantified from comparison with reference in situ or other suitable reference data. Uncertainties are characterised in a statistically robust way over multiple locations and time periods representing global conditions. Spatial and temporal consistency of the product and consistency with similar products has been evaluated over globally representative locations and periods. Results are published in the peer-reviewed literature.
Stage 4	Validation results for stage 3 are systematically updated when new product versions are released and as the time-series expands.

5.2 A General Validation Strategy

A general validation strategy should be capable of testing products for compliance with GCOS requirements. A distinction is made between the strategy, corresponding to a sampling design, a definition of key reference datasets, and inter-comparison methods, versus the data required for use with this strategy in order to test if the satellite products meet either threshold or science requirements. The major criteria of the validation strategy are detailed in the following sub-sections:

5.2.1 Validation on a globally- and seasonally-representative basis

Direct validation relies on reference datasets traceable to *in situ* reference measurements accompanied by an associated assessment of their uncertainty. Reference *in situ* surface albedo data should take into account the spatial variability and representativeness of the *in-situ* measurements and scaling should be performed if necessary. Up-scaling methods (for heterogeneous sites) should be based on higher resolution information of the surface spatial variability using not only surface albedo but auxiliary variables such as land cover maps and/or high-resolution satellite/airborne imagery. Matchups of spatially and temporally coincident products and reference values should be compared using appropriately robust statistics and the visualization of residuals. Validation results should be provided for each season separately (e.g. vegetation growing season, dormant period, and snow-covered period) and they should be stratified by class for the ancillary data (e.g. according to land cover type).

5.2.2 Quantify the representativeness of surface albedo accuracy estimates over areas or time periods without reference datasets

There are three issues with representativeness.

1. The precision of the accuracy estimate assuming the reference data are globally representative.
2. The spatial extent of the comparison.
3. The temporal domain that the comparison applies to.

Ideally, albedo should be rigorously evaluated using a time series of globally distributed reference datasets of sufficient length, consistency, and continuity to adequately meet the science requirements. An evaluation of albedo products at the global scales can be done using albedo products inter-comparisons, but this method does not represent a complete and independent validation. A full set of uncertainty estimates of albedo products mentioned in Section 3.3 can be used to quantify the representativeness of accuracy statistics over areas or time periods without reference datasets. The representativeness of accuracy can also be quantified by comparing the albedo products with the albedo that have been evaluated using reference datasets with the same land cover and seasonal conditions.

5.2.3 Stability Evaluation

The evaluation of the retrieved albedo stability is performed analysing specific regions on Earth, using statistical approach. This analysis is not a validation but it can offer a robust indication of the degree of reliability of an albedo dataset. The most indicated areas for this evaluation are bright desert areas. Such areas are supposed to experience very little variations during the years. This is a very strong assumption and it is also not always easy to verify due to the remote and not easily accessible location of these desertic regions. Some examples of target areas for stability evaluation are in Libya and Egypt. A list of these and other targets can be found in the Surface Albedo

Validation Sites (SAVS) list (DOI: http://dx.doi.org/10.15770/EUM_SEC_CLM_1001) [*Loew et al. 2016*]. The following procedure should be considered:

- Select at least 3 areas sensed with different viewing angles (for Geostationary platform at least);
- Define a 3x3 and 5x5 pixels area around the target nominal location;
- Estimate the average (AVG) and standard deviation (STDEV) of the retrieved albedo;
- Plot the time series of AVG using STDEV as uncertainty if no other is available;
- Estimate the regression slope and compare with the 15/decade GCOS requirement.

Examples of stability evaluation can be found in [*Fell et al. 2012*].

5.3 Status of Current Validation Capacity and Methods

5.3.1 Methods

Multiple validation methods are necessary to characterize the product uncertainties and to assess the compliance of albedo products with user requirements. Three different methods have been widely used to validate and determine surface albedo satellite product uncertainties: ground-based validation, product inter-comparison and upscaling pixel-to-pixel validation.

The goal of this section to provide guidelines for producing statistics related to the accuracy, precision and completeness of surface albedo products with global coverage. Accuracy estimates require comparison of corresponding product and reference surface albedo values.

5.3.1.1 Ground-based validation

This approach involves comparisons with *in-situ* tower-based albedo measurements, and have been frequently used to validate albedo products retrieved from MODIS [*Liu et al.*, 2009; *Cescatti et al.*, 2012; *Wang et al.*, 2012, 2014], Multi-angle Imaging SpectroRadiometer (MISR) [*Chen et al.*, 2008], POLDER [*Hautecoeur and Roujean*, 2007], VIIRS [*Liu et al.*, 2017], Advanced Very High Resolution Radiometer (AVHRR) [*Sütterlin et al.*, 2015], SEVIRI [*Carrer et al.*, 2010; *Carrer et al.,* 2018a], Landsat [*Shuai et al.,* 2011, 2014; *Wang et al*., 2017], Sentienel-2 [*Li et al.,* 2018]. The main limitation of this approach is the spatial representativeness of the *in situ* reference measurements. Reference albedo measured from towers cover a circular footprint that varies with tower height. It is unlikely that the footprint of the ground measurements matches exactly with the satellite pixel sizes. The spatial representativeness of ground albedo measurements will depend on the land surface heterogeneity. Ground measurements with smaller footprints can only be used to evaluate satellite data with larger pixel sizes over homogeneous surfaces. Large differences between the two datasets should be expected over areas with heterogeneous surfaces. A spatial representativeness analysis (Figure 3) is necessary for satellite albedo validation using tower-based albedo, in particular for cases when the tower footprint size is larger than the spatial resolution of albedo products [*Román et al.*, 2009; *Wang et al.*, 2012, 2014].

The semivariogram [*Matheron*, 1963; *Davis*, 1986; *Isaaks and Srivastava*, 1989; *Carroll and Cressie*, 1996] is one of the most efficient tools for describing spatial representativeness. The characteristics of semivariograms (e.g. the sill, range, and nugget) can reveal the spatial variability of land surfaces and reveal the scaling effects associated with remotely sensed data [*Woodcock et al.*, 1988a, 1988b; *Román et al.*, 2009, 2010, *Wang et al.*, 2012, 2014, 2017]. Semivariograms can be estimated from 30-m spatial resolution near-nadir Landsat or Sentinel-2 surface reflectances at different periods of the year to check for the spatial representativeness of the region around the ground tower.

$$\gamma_E(h) = 0.5 \cdot \frac{\sum_{i=1}^{N(h)} (z_{xi} - z_{xi+h})^2}{N(h)} \tag{8}$$

where $\gamma_E(h)$ is the variogram estimator between reflectances that are within certain distance; z_{xi} is the surface reflectance at pixel location x; z_{xi+h} is the surface reflectance of another pixel within a lag distance h, and $N(h)$ is the number of paired data at a distance of h.
The spatial attributes (range, sill and nugget) can then be modified to fit a spherical model [*Matheron*, 1963] to the variogram estimator:

$$\gamma_{sph}(h) = \begin{cases} c_0 + c \cdot (1.5 \cdot \frac{h}{a} - 0.5(\frac{h}{a})^3) & for\ \ 0 \le h \le a \\ c_0 + c & for\ \ h > a \end{cases} \tag{9}$$

Where the range (a) describes the average patch size of the landscape [*Cooper et al.*, 1997], and is the distance at which there is no further correlation of biophysical property associated with a point. The sill (c) describing the maximum semivariance, is the ordinate value of the range at which the variogram levels off to an asymptote. The nugget (c_0) describes variance at h=0, which may be nonzero. It depends on the variance associated with small scale variability, measurement errors, or a combination of these [*Noréus et al.*, 1997].

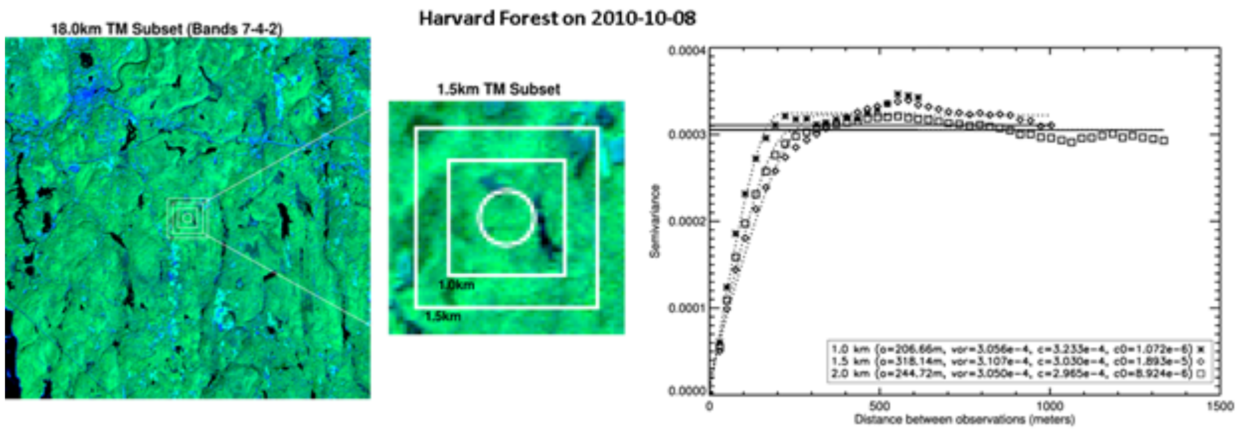

Figure 3. Top-of-Atmosphere (TOA) shortwave reflectance composite (TM Bands 7–4–2) and corresponding semivariogram functions, variogram estimator (points), spherical model (dotted curves), and sample variance (solid straight lines) using regions of 1.0 km (asterisks), 1.5 km (diamonds), and 2.0 km (squares), centered over the Harvard Forest site on 2010-10-08. The size of the circle in the center image (footprint of tower albedo measurements) is calculated based on the height at which the albedometer is mounted and the albedometer FOV (Figure from Wang et al., 2017).

The comparison between *in situ* albedo with satellite albedo products should be performed for all seasons especially for the seasonal transition periods (spring and autumn) to evaluate the accuracy of albedo products over different conditions (e.g. leaf-on, leaf-off, snow-covered, snow-free).

5.3.1.2 Satellite Product Inter-comparison

The inter-comparison of products offers a means of assessing the discrepancies (systematic or random) between products. This method involves comparing satellite albedo products with each other, particularly new products with heritage albedo products [*Carrer et al.*, 2010; *Carrer et al.,* 2018a; *Taberner et al.*, 2010; *Wang et al.*, 2013; *Sütterlin et al.*, 2015; *Liu et al.*, 2017, *Fell et al.* 2012]. This method is particularly valuable for finding spatial disagreements between albedo products over large areas and for a wide range of cover types. However, this approach does not yield absolute validation results and satellite albedo inter-comparisons alone are insufficient to validate a new product. The inter-comparison approach must account for differences in the spatial resolution between the satellite datasets. Liu et al. (2017) compared the VIIRS albedo product with the MODIS albedo product. The majority of the broadband shortwave (high quality) albedo values lies along the 1:1 line and falls within the ±0.025 boundary (Figure 4) over three distributed MODIS tiles.

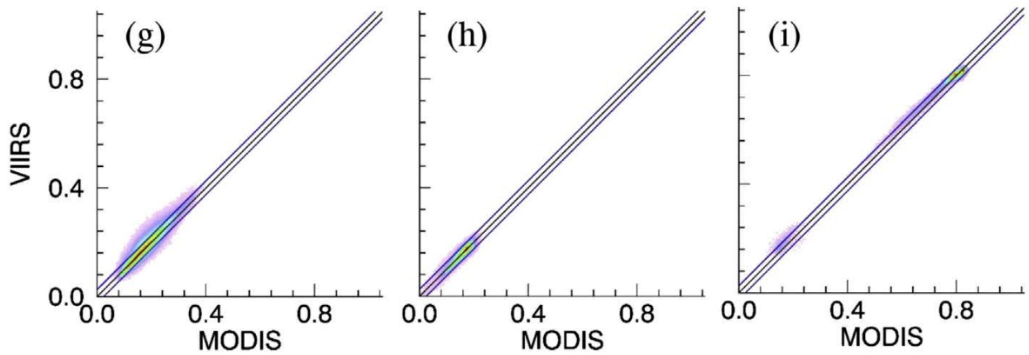

Figure 4. MODIS and VIIRS broadband shortwave albedo over tiles h08v05 (g), h11v04 (h), and h16v02 (i). Red indicates high density and light purple indicates low density [*Liu et al*., 2017].

Spatial consistency refers to the realism and repeatability of the spatial distribution of retrievals over the globe. The spatial discrepancies between albedo products can be quantitatively assessed by comparing the spatial distribution of a reference validated product with the albedo satellite product under study. Two products are considered spatially consistent when the residual lays within uncertainty requirements of the variable. The residual (ε) is estimated assuming a linear trend between two products (Y = a X+ b + ε). The residual represents the remaining discrepancies regarding the general trend between both products. In this way, systematic trends are not considered depicting more clearly patterns associated to the spatial distribution of retrievals. The spatial discrepancies between PROBA-V surface albedo products and SPOT/VGT albedo products (Figure 5) were evaluated to assess the continuity of the albedo products in the Copernicus Global Land Service (*Carrer et al.,* 2018b; *Sánchez-Zapero et al*., 2018b).

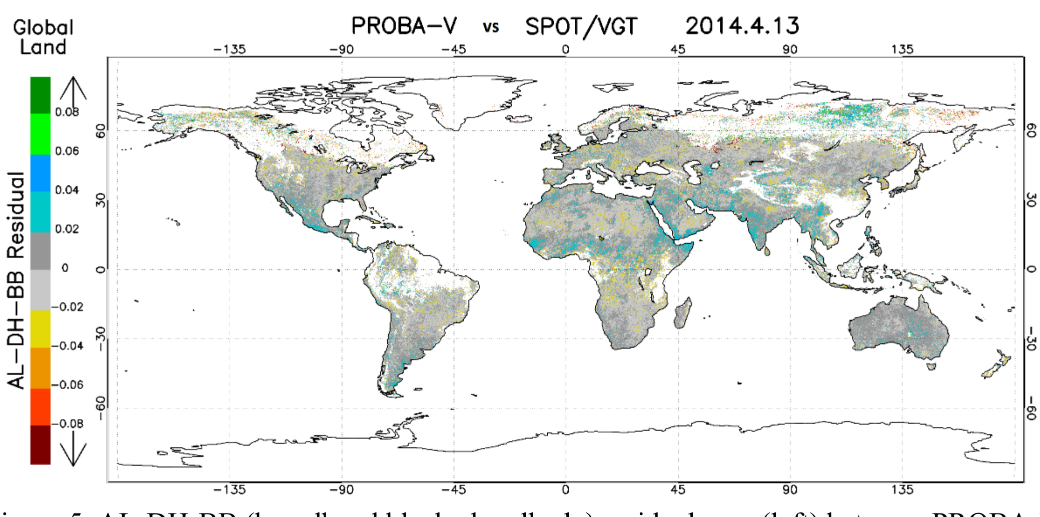

Figure 5. AL-DH-BB (broadband black-sky albedo) residual map (left) between PROBA-V and SPOT/VGT SA V1.5 for 13th April, 2014. (Figure from Sánchez-Zapero et al., 2018b).

The Surface Albedo Validation Sites (SAVS) catalogue [*Fell et al., 2015; Loew et al., 2016]* , available on the EUMETSAT website (http://savs.eumetsat.int), characterizes more than 2000 sampling stations around the world that provide either albedo reference measurements for direct comparison, or atmospheric state measurements useful for correlation and inter-comparison of satellite derived surface albedos. Analysing a number of ancillary datasets, the SAVS database provides metrics on the spatio-temporal representativeness of each site, the temporal stability, as well as the topographic and land cover homogeneity of each site [*Román et al., 2009; Loew et al., 2016]*. An example of the use of such information for the selection of relevant sites for application to geostationary satellite products validation is shown on Figure 6.

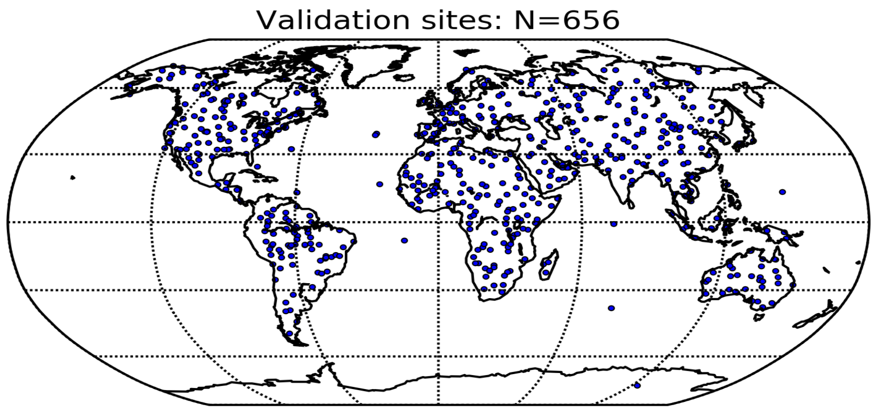

Figure 6. Location of the most suitable potential validation sites for geostationary-derived albedo products, identified from the EUMETSAT Surface Albedo Validation Sites (SAVS), based on Fell et al. [*2015*] criteria.

Based on an optimal subset of the SAVS validation sites plus desertic calibration sites, a Surface Albedo Validation (SALVAL) tool [*de la Madrid et al., 2018*] was developed in the framework of the Copernicus Climate Change Service to provide transparency and traceability to the validation and inter-comparison process of albedo products. SALVAL tool allows to evaluate different quality criteria by product comparison, such as product completeness, spatial and temporal consistency, precision and provide an overall statistical analysis of discrepancies between albedo products. The product completeness can be evaluated by the spatial distribution of the percentage of missing values (Figure 7), temporal evolution of missing values, and temporal length of a missing values [*Sánchez-Zapero et al., 2018a*].

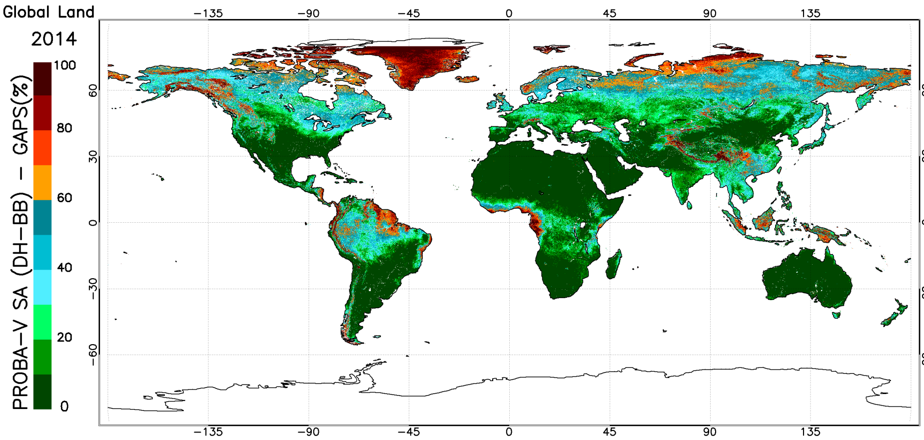

Figure 7. Percentage of missing values during the January-December 2014 period for PROBA-V AL-DH-BB product considering all land pixels. (Figure from Sánchez-Zapero et al., 2018b)

The realism and stability of the temporal variations or temporal consistency of a new albedo product can be qualitatively analysed as compared to reference validated albedo products. Figure 8 reveals a good inter-annual consistency of albedo temporal variations over a Needle Leaf site, whereas over a desertic site in Libya a large seasonality is displayed in the SPOT/VGT albedo product which is not depicted in MODIS and GLASS products and corresponds to a bug in the Earth-Sun distance correction of the SPOT/VGT collection 2 archive which was fixed in collection 3.

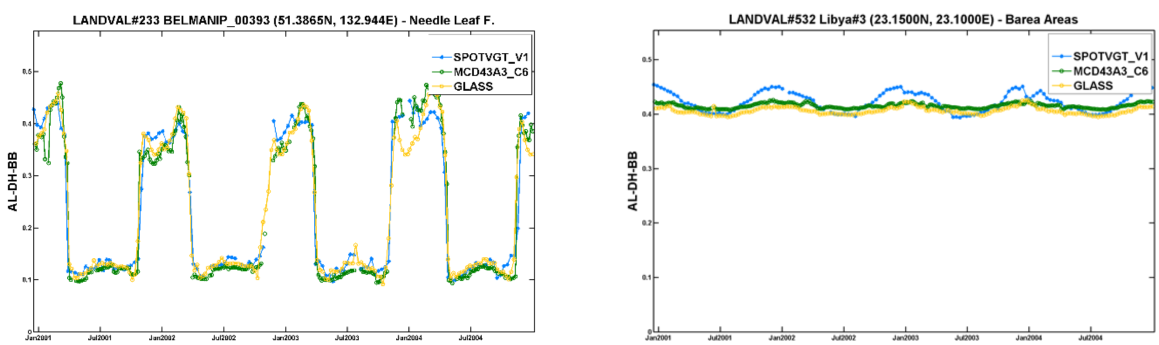

Figure 8. Temporal variations of SPOT/VGT V1, MODIS MCD43A3 C6 and GLASS AL-DH-BB retrievals during the 2000-2005 period over two selected LANDVAL sites. Needle-Leaf forest on the left side, and Bare Areas on the right side. From (Sánchez-Zapero et al., 2018a).

5.3.1.3 Upscaling high spatial resolution airborne/spaceborne albedo

This approach involves validating coarse spatial resolution albedo products by aggregating high spatial resolution airborne/spaceborne albedo reference data to the spatial resolution of the coarse product, in particular over heterogeneous surfaces. The accuracy of high spatial resolution airborne/spaceborne albedo estimates should themselves be first validated using *in situ* albedo measurements. Román et al. (2013) utilized airborne albedo estimates retrieved from multi-angular observations from NASA's CAR to evaluate the MODIS albedo product. Multi-angular airborne reflectance measurements can also be used to evaluate the albedo models by comparing airborne angular observations with the model simulated angular reflectance.

5.3.2 Challenges to Validation Strategy

5.3.2.1 Insufficient reference datasets

Although, current albedo reference datasets cover many land surface types, the number of *in situ* albedo sites is still globally limited and does not cover all kinds of surface conditions. It remains a challenge to validate albedo products over heterogenous areas due to insufficient distribution of reference datasets.

5.3.2.2 Thematic Differences in Albedo Definitions

Currently most surface albedo products do not directly produce the actual blue-sky albedo that is measured directly by in-situ pyranometers. Further processing steps (e.g. generation of blue-sky from black-sky and white-sky albedo) are needed that are based on actual atmospheric conditions. Differences in the definitions of quantities represented in the currently available albedo products have led to substantial variability across performance assessments. Acceptable products should be compared to reference surface albedo datasets corresponding to the actual blue-sky albedo values as defined by GCOS.

5.3.2.3 Use of Quality Flags and Uncertainty

Many products provide the quality flags and uncertainty values associated with the albedo values that need to be considered during the validation. It is recommended to evaluate the accuracy of albedo with different level of quality.

5.3.3 Reporting Results of Surface Albedo Validation

5.3.3.1 Validation Metrics

Definitions of the accuracy, precision, uncertainty, and completeness applicable to surface albedo validation are drawn from experimental statistics which are provided in Section 2.4. As a best practice, validation exercises should explicitly define these terms and identify how they relate to the definitions provided in Section 2.4 to facilitate an understanding of results across studies. Surface albedo product validation should be performed across a representative sampling of surface albedo magnitudes within spatial and temporal stratifications. It is also a good practice to evaluate the precision and completeness of spatial and temporal patterns, in addition to reporting the statistics based on surface albedo product estimates in a stratum without spatial or temporal considerations. Table 3 summarizes the common practices and recommended best practices.

Table 3. Common practice and recommended good practice.

Quantity	Current practice	Good practice, add:
Accuracy	Bias; absolute bias	Median error Median and percentiles of residuals Box-plots of residuals vs. Albedo
Precision	Standard deviation	Median absolute deviation Median 3 point difference
Uncertainty	Root mean square error	Scatter plot of match-ups Median and percentiles of absolute residuals, RMSE Box-plots of absolute residuals vs. Albedo
Completeness		Gap size distribution Gap length
Stability		Time series average, standard deviation, and regression slope Mean error per decade

5.3.3.2 Stratification of Performance Statistics

Surface albedo products provide time-series datasets so that a complete validation should ideally include comparison of the spatial and temporal patterns of albedo. This involves two additional degrees of freedom over which reference samples must be acquired (beyond simply considering the mean albedo magnitude over a given location over time). Product precision and consistency can and should include these considerations. To avoid confusion due to differences in the stratification used for accuracy, precision and completeness it is recommended that assessments are constrained to a single stratification.

It is a good practice to employ a spatial stratification for performance assessments which correspond to the continental biomes used in current albedo algorithms together with a temporal stratification separated into at least snow-free and snow-covered conditions.

It is a good practice to sample across a representative range of albedo values within a stratification to obtain all performance statistics.

It is a good practice to evaluate the precision and completeness of spatial and temporal patterns in addition to simply reporting the statistics based on albedo product estimates in a stratum without spatial or temporal considerations.

5.3.3.3 Reporting validation results

The results of validation exercises should be reported publicly after review by the data producers and after independent scientific peer review. Reporting in refereed journals are encouraged and supporting materials corresponding to spatial or temporal accuracy statistics should be accessible. The following details are related to reporting best practices:

1) All participants in the exercise should be declared unless products were provided blindly.

2) Links to accessible versions of the products and reference data used during the validation should be provided and maintained.

3) Match-ups of the product and reference surface albedo values used to derive aggregation statistics together with ancillary information related to location (at least for the continent and biome), temporal interval (at least snow or snow free condition), and uncertainty in reference data (at least a reference to the protocol used to produce each reference data point) should all be made available publicly.

4) Statistics should be reported within the validation document or linked to supplementary material in addition to any other statistics.

6 CONCLUSIONS

This document provides recommendations on the best practices that should be used for the validation of satellite derived albedo products. Validation efforts should include a full characterization and appropriate documentation of the validation datasets used, including the uncertainty estimates of reference albedo measurements. The spatial representativeness of tower-based albedo measurements should be provided for those cases where the footprint of the tower-based albedo values is smaller than the pixel size of satellite albedo products. It is recommended that only sites that are spatially representative of the satellite field of view should be used for validation purposes. These can include sites which have a fairly uniform cover or sites which have a fairly broad area of heterogenous cover types. Three albedo validation approaches have been identified: (1) ground-based validation, which involves comparisons with spatially representative tower-based albedo measurements; (2) indirect validation, consisting of inter-comparisons of satellite-derived albedo products over common spatial and temporal supports, and (3) upscaling validation, which evaluates albedo products using higher spatial resolution albedo datasets from airborne or satellite estimates. The availability of reference albedo datasets is fundamental for validation efforts: currently, albedo validation sites are only sufficient to allow a CEOS Level 3 validation stage (Table 2).

7 REFERENCES

Augustine, J. A., J. J. DeLuisi, and C. N. Long (2000), SURFRAD—A National Surface Radiation Budget Network for Atmospheric Research, *Bull. Am. Meteorol. Soc.*, doi:10.1175/1520-0477(2000)081<2341:SANSRB>2.3.CO;2.

Baldocchi, D. et al. (2001), FLUXNET: A New Tool to Study the Temporal and Spatial Variability of Ecosystem-Scale Carbon Dioxide, Water Vapor, and Energy Flux Densities, *Bull. Am. Meteorol. Soc.*, *82*(11), 2415–2434, doi:10.1175/1520-0477.

Baret, F., C. Schaaf, J. Morisette, and J. Privette (2005), Report on the Second International Workshop on Albedo Product Validation, *Earth Obs.*, *17*, 13–17.

Campagnolo, M. L., Q. Sun, Y. Liu, C. Schaaf, Z. Wang, and M. O. Román (2016), Estimating the effective spatial resolution of the operational BRDF, albedo, and nadir reflectance products from MODIS and VIIRS, *Remote Sens. Environ.*, *175*, 52–64, doi:10.1016/j.rse.2015.12.033.

Carrer, D., J. L. Roujean, and C. Meurey (2010), Comparing operational MSG/SEVIRI Land Surface albedo products from Land SAF with ground measurements and MODIS, *IEEE Trans. Geosci. Remote Sens.*, doi:10.1109/TGRS.2009.2034530.

Carrer, D., S. Moparthy, G. Lellouch, X. Ceamanos, F. Pinault, S.C. Freitas, I.F. Trigo (2018a), Land Surface Albedo Derived on a Ten Daily Basis from Meteosat Second Generation Observations: The NRT and Climate Data Record Collections from the EUMETSAT LSA SAF. *Remote Sens.*, 10, 1262.

Carrer, D., B. Smets, X. Ceamanos, J.-L. Roujean, R. Lacaze (2018b), Copernicus Global Land SPOT/VEGETATION and PROBA-V Surface Albedo Products—1 Km Version 1; Algorithm Theoretical Basis Document, Issue 2.11, *Copernicus Global Land Operations Vegetation and Energy CGLOPS-1. Framework Service Contract* N° 199494; JRC

Carroll, S. S., and N. Cressie (1996), A comparison of geostatistical methodologies used to estimate snow water equivalent, *Water Resour. Bull.*, *32*, 267–278, doi:10.1111/j.1752-1688.1996.tb03450.x.

Cescatti, A. et al. (2012), Intercomparison of MODIS albedo retrievals and in situ measurements across the global FLUXNET network, *Remote Sens. Environ.*, doi:10.1016/j.rse.2012.02.019.

Chen, Y. M., S. Liang, J. Wang, H. Y. Kim, and J. V. Martonchik (2008), Validation of MISR land surface broadband albedo, *Int. J. Remote Sens.*, doi:10.1080/01431160802199876.

Cooper, S. D., L. Barmuta, O. Sarnelle, K. Kratz, and S. Diehl (1997), Quantifying spatial heterogeneity in streams, *J. North Am. Benthol. Soc.*, doi:10.2307/1468250.

Davis, J. C. (1986), *Statistics and Data Analysis in Geology*.

de la Madrid, L., Sánchez-Zapero, J., Camacho, F. (2018). SALVAL: a semi-automatic Surface ALbedo VALidation tool. *Worskshop on Land Product Validation and Evolution (LPVE 2018).* 27 Feb. - 1Mar. 2018, ESA-ESRIN, Frascati (Rome), Italy.

Fell F., Bennartz R., Cahill B. , Lattanzio Alessio., Muller J.P. , Schulz J., Shane N., Trigo I., Watson G. (2012) Evaluation of the Meteosat Surface Albedo Climate Data Record (ALBEDOVAL) Final Report V1.1

Fell, F., R. Bennartz, and A. Loew (2015), *Validation of the EUMETSAT Geostationary Surface Albedo Climate Data Record -2- (ALBEDOVAL-2) Final report V1.1*.

Fernandes, R. et al. (2014), *Global Leaf Area Index Product Validation Good Practices. Version 2.0. In G. Schaepman-Strub, M. Román, & J. Nickeson (Eds.), Best Practice for Satellite-Derived Land Product Validation (p. 76): Land Product Validation Subgroup (WGCV/CEOS)*.

GCOS-107 (2006), *Systematic Observation Requirements for Satellite-based Products for Climate - GCOS-107 (WMO/TD No. 1338)*.

GCOS-138 (2010), *Implementation plan for the global observing system for climate in support of the UNFCCC*.

GCOS-154 (2011), *Systematic Observation Requirements For Satellite-Based Data Products for Climate - 2011 Update*.

GCOS-200 (2016), The Global Observing System for Climate: Implementation Needs (GCOS-200),

GCOS-92 (2004), *IMPLEMENTATION PLAN FOR THE GLOBAL OBSERVING SYSTEM FOR CLIMATE IN SUPPORT OF THE UNFCCC*.

Geiger, B., D. Carrer, L. Franchistéguy, J. L. Roujean, and C. Meurey (2008), Land surface albedo derived on a daily basis from meteosat second generation observations, *IEEE Trans. Geosci. Remote Sens.*, doi:10.1109/TGRS.2008.2001798.

Govaerts, Y. M., and A. Lattanzio (2007), Retrieval error estimation of surface albedo derived from geostationary large band satellite observations: Application of Meteosat-2 and Meteosat-7 data, *J. Geophys. Res. Atmos.*, *112*(5), 1–12, doi:10.1029/2006JD007313.

Govaerts, Y. M., B. Pinty, M. Taberner, and A. Lattanzio (2006), Spectral conversion of surface albedo derived from meteosat first generation observations, *IEEE Geosci. Remote Sens. Lett.*, doi:10.1109/LGRS.2005.854202.

GUM-2008 (2008), Evaluation of measurement data — Guide to the expression of uncertainty in measurement, *Int. Organ. Stand. Geneva ISBN*, *50*(September), 134, doi:10.1373/clinchem.2003.030528.

Hamilton, M. P., E. a. Graham, P. W. Rundel, M. F. Allen, W. Kaiser, M. H. Hansen, and D. L. Estrin (2007), New Approaches in Embedded Networked Sensing for Terrestrial Ecological Observatories, *Environ. Eng. Sci.*, *24*(2), 192–204, doi:10.1089/ees.2006.0045.

Hautecoeur, O., and J. L. Roujean (2007), Validation of POLDER surface albedo products based on a review of other satellites and climate databases, in *International Geoscience and Remote Sensing Symposium (IGARSS)*.

Isaaks, E. H., and R. M. Srivastava (1989), *An introduction to applied geostatistics*, New York Oxford University Press.

Kampe, T. U. (2010), NEON: the first continental-scale ecological observatory with airborne remote sensing of vegetation canopy biochemistry and structure, *J. Appl. Remote Sens.*, *4*(1), 043510, doi:10.1117/1.3361375.

Lattanzio, A., Fell, F., Bennartz, R., Trigo, I. F., and Schulz, J.: Quality assessment and improvement of the EUMETSAT Meteosat Surface Albedo Climate Data Record, *Atmos. Meas. Tech*., 8, 4561-4571, https://doi.org/10.5194/amt-8-4561-2015, 2015

Lebourgeois, F., J. C. Pierrat, V. Perez, C. Piedallu, S. Cecchini, and E. Ulrich (2010), Simulating phenological shifts in French temperate forests under two climatic change scenarios and four driving global circulation models, *Int. J. Biometeorol.*, doi:10.1007/s00484-010-0305-5.

Levy, C., E. Burakowski, A. Richardson (2018), Novel measurements of fine-scale albedo: Using a commercial quadcopter to measure radiation fluxes. *Remote Sens.*, 10, 1303

Lewis, P., and M. Barnsley (1994), Influence of the sky radiance distribution on various formulations of the earth surface albedo, *Proc. Conf. Phys. Meas. Signatures Remote Sens.*, 707–715.

Li, X., and Strahler, A.H.(1986), Geometric-optical bidirectional reflectance modeling of a conifer forest canopy, *IEEE Trans. Geosci. Remote Sens*., GE-24, 906–919.

Li, X., and Strahler, A.H.(1992), Geometric-optical bidirectional reflectance modeling of the discrete crown vegetation canopy: Effect of crown shape and mutual shadowing. *IEEE Trans. Geosci. Remote Sens.*, 30, 276–292

Li, Z., A. Erb, Q. Sun, Y. Liu, Y. Shuai, Z. Wang, P. Boucher, and C. Schaaf (2018), Preliminary assessment of 20-m surface albedo retrievals from sentinel-2A surface reflectance and MODIS/VIIRS surface anisotropy measures, *Remote Sens. Environ.*, *217*(August), 352–365, doi:10.1016/j.rse.2018.08.025.

Liang, S. (2001), Narrowband to broadband conversions of land surface albedo I Algorithms, *Remote Sens. Environ.*, *76*, 213–238.

Liang, S., C. J. Shuey, A. L. Russ, H. Fang, M. Chen, C. L. Walthall, C. S. T. Daughtry, and R. Hunt (2003), Narrowband to broadband conversions of land surface albedo: II. Validation, *Remote Sens. Environ.*, doi:10.1016/S0034-4257(02)00068-8.

Liang, S. A. H. S. C. W. (1999), Retrieval of Land Surface Albedo from Satellite Observations: A Simulation Study, *J. Appl. Meteorol.*, *38*, 712–725, doi:10.1175/1520-0450(1999)038<0712:ROLSAF>2.0.CO;2.

Liu, J., C. Schaaf, A. Strahler, Z. Jiao, Y. Shuai, Q. Zhang, M. Roman, J. A. Augustine, and E. G. Dutton (2009), Validation of Moderate Resolution Imaging Spectroradiometer (MODIS) albedo retrieval algorithm: Dependence of albedo on solar zenith angle, *J. Geophys. Res.*, *114*, doi:10.1029/2008JD009969.

Liu, Y. et al. (2017), Evaluation of the VIIRS BRDF, Albedo and NBAR products suite and an assessment of continuity with the long term MODIS record, *Remote Sens. Environ.*, doi:10.1016/j.rse.2017.09.020.

Loew, A. (2014), Terrestrial satellite records for climate studies: How long is long enough? A test case for the Sahel, *Theor. Appl. Climatol.*, doi:10.1007/s00704-013-0880-6.

Loew, A., R. Bennartz, F. Fell, A. Lattanzio, M. Doutriaux-Boucher, and J. Schulz (2016), A database of global reference sites to support validation of satellite surface albedo datasets (SAVS 1.0), *Earth Syst. Sci. Data*, doi:10.5194/essd-8-425-2016.

Lucht, W., and P. Lewis (2000), Theoretical noise sensitivity of BRDF and albedo retrieval from the EOS-MODIS and MISR sensors with respect to angular sampling, *Int. J. Remote Sens.*, *21*(1), 81–98.

Lucht, W., C. B. Schaaf, and a. H. Strahler (2000), An algorithm for the retrieval of albedo from space using semiempirical BRDF models, *IEEE Trans. Geosci. Remote Sens.*, *38*(2), 977–998, doi:10.1109/36.841980.

Lyapustin, A. et al. (2014), Scientific impact of MODIS C5 calibration degradation and C6+ improvements, *Atmos. Meas. Tech.*, doi:10.5194/amt-7-4353-2014.

Matheron, G. (1963), Principles of geostatistics, *Econ. Geol.*, doi:10.2113/gsecongeo.58.8.1246.

McArthur, L. B. J. (2005), *Baseline Surface Radiation Network (BSRN)Operations Manual Version 2.1WCRP-121*.

Michalsky, J. J., L. C. Harrison, and W. E. Berkheiser (1995), Cosine response characteristics of some radiometric and photometric sensors, *Sol. Energy*, doi:10.1016/0038-092X(95)00017-L.

Mishra, N., D. Helder, A. Angal, J. Choi, and X. Xiong (2014), Absolute calibration of optical satellite sensors using libya 4 pseudo invariant calibration site, *Remote Sens.*, doi:10.3390/rs6021327.

Müller, R. (2014), Calibration and verification of remote sensing instruments and observations, *Remote Sens.*, doi:10.3390/rs6065692.

Noréus, J. P., M. R. Nyborg, and K. L. Hayling (1997), The gravity anomaly field in the Gulf of Bothnia spatially characterized from satellite altimetry and in situ measurements, *J. Appl. Geophys.*, doi:10.1016/S0926-9851(97)00007-4.

Ohmura, A. et al. (1998), Baseline Surface Radiation Network (BSRN/WCRP): New Precision Radiometry for Climate Research, *Bull. Am. Meteorol. Soc.*, *79*(10), 2115–2136, doi:10.1175/1520-0477(1998)079<2115:BSRNBW>2.0.CO;2.

Ohring, G., B. Wielicki, R. Spencer, B. Emery, and R. Datla (2004), *Satellite Instrument Calibration for Measuring Global Climate Change Report of a Workshop in 2002*.

Pinty, B., F. Roveda, M. M. Verstraete, N. Gobron, Y. Govaerts, J. V. Martonchik, D. J. Diner, and R. A. Kahn, 2000a: Surface albedo retrieval from Meteosat 1. Theory. J. Geophys. Res., 105(D14), 18 099–18 112.

Pinty, B., F. Roveda, M. M. Verstraete, N. Gobron, Y. Govaerts, J. V. Martonchik, D. J. Diner, and R. A. Kahn, 2000b: Surface albedo retrieval from Meteosat 2. Applications. J. Geophys. Res., 105(D14), 18 113–18 134.

Pinty, B., J. L. Widlowski, N. Gobron, M. M. Verstraete, and D. J. Diner (2002), Uniqueness of multiangular measurements - Part I: An indicator of subpixel surface heterogeneity from MISR, *IEEE Trans. Geosci. Remote Sens.*, doi:10.1109/TGRS.2002.801148.

Pinty, B., A. Lattanzio, J. V. Martonchik, M. M. Verstraete, N. Gobron, M. Taberner, J.-L. Widlowski, R. E. Dickinson, and Y. Govaerts (2005), Coupling Diffuse Sky Radiation and Surface Albedo, *J. Atmos. Sci.*, doi:10.1175/JAS3479.1.

Pirazzini, R. (2004), Surface albedo measurements over Antarctic sites in summer, *J. Geophys. Res. D Atmos.*, *109*, doi:10.1029/2004JD004617.

Pirazzini, R., T. Vihma, M. A. Granskog, and B. Cheng (2006), Surface albedo measurements over sea ice in the Baltic Sea during the spring snowmelt period, in *Annals of Glaciology*, vol. 44, pp. 7–14.

Planque, C., D. Carrer, and J. L. Roujean (2017), Analysis of MODIS albedo changes over steady woody covers in France during the period of 2001–2013, *Remote Sens. Environ.*, doi:10.1016/j.rse.2016.12.019.

Rahman, H.; Verstraete, M.M.; Pinty, B. Coupled Surface-Atmosphere Reflectance (CSAR) model 1. Mmodel description and inversion on synthetic data. J. Geophys. Res. 1993, 98, 20779-20789

Roesch, A., and E. Roeckner (2006), Assessment of snow cover and surface albedo in the ECHAM5 general circulation model, *J. Clim.*, doi:10.1175/JCLI3825.1.

Román, M. O. et al. (2009), The MODIS (Collection V005) BRDF/albedo product: Assessment of spatial representativeness over forested landscapes, *Remote Sens. Environ.*, doi:10.1016/j.rse.2009.07.009.

Román, M. O., C. B. Schaaf, P. Lewis, F. Gao, G. P. Anderson, J. L. Privette, A. H. Strahler, C. E. Woodcock, and M. Barnsley (2010), Assessing the coupling between surface albedo derived from MODIS and the fraction of diffuse skylight over spatially-characterized landscapes, *Remote Sens. Environ.*, *114*(4), 738–760, doi:10.1016/j.rse.2009.11.014.

Román, M. O., C. K. Gatebe, C. B. Schaaf, R. Poudyal, Z. Wang, and M. D. King (2011), Variability in surface BRDF at different spatial scales (30m-500m) over a mixed agricultural landscape as retrieved from airborne and satellite spectral measurements, *Remote Sens. Environ.*, *115*, 2184–2203, doi:10.1016/j.rse.2011.04.012.

Román, M. O., C. K. Gatebe, Y. Shuai, Z. Wang, F. Gao, J. G. Masek, T. He, S. Liang, and C. B. Schaaf (2013), Use of in situ and airborne multiangle data to assess MODIS- and landsat-based estimates of directional reflectance and albedo, *IEEE Trans. Geosci. Remote Sens.*, *51*, 1393–1404, doi:10.1109/TGRS.2013.2243457.

Ross, J. (1981), The Radiation Regime and Architecture of Plant Stands; *Dr. W. Junk: Norwell, MA, USA.*

Roujean, J.-L. J.-L., M. Leroy, D. P-Y, and P.-Y. Deschamps (1992), A Bidirectional Reflectance Model of the Earth's surface for the Correction of Remote Sensing Data, *J. Geophys. Res.*, *97*, 20455–20468.

Sánchez-Zapero, J., Camacho, F., de la Madrid, L., Wang, Z., Roman, M.O. (2018a). Validation and Inter-Comparisson of four global surface albedo products using the SALVAL tool. *Worskshop on Land Product Validation and Evolution (LPVE 2018).* 27 Feb. - 1Mar. 2018, ESA-ESRIN, Frascati (Rome), Italy.

Sánchez-Zapero, J., de la Madrid, L., Camacho, F. (2018b). Validation Report of Surface Albedo from PROBA-V Collection 1km Version 1.5 (p. 122). *Copernicus Global Land Operations - Lot1. Framework Service Contract Nº 199494 (JRC).*

Schaepman-Strub, G., M. E. Schaepman, T. H. Painter, S. Dangel, and J. V. Martonchik (2006), Reflectance quantities in optical remote sensing-definitions and case studies, *Remote Sens. Environ.*, doi:10.1016/j.rse.2006.03.002.

Schimel, D., W. Hargrove, F. Hoffman, and J. MacMahon (2007), NEON: a hierarchically designed national ecological network, *Front. Ecol. Environ.*, *5*(2), 59–59, doi:10.1890/1540-9295(2007)5[59:NAHDNE]2.0.CO;2.

Shuai, Y., C. B. Schaaf, A. H. Strahler, J. Liu, and Z. Jiao (2008), Quality assessment of BRDF/albedo retrievals in MODIS operational system, *Geophys. Res. Lett.*, *35*, doi:10.1029/2007GL032568.

Shuai, Y., J. G. Masek, F. Gao, and C. B. Schaaf (2011), An algorithm for the retrieval of 30-m snow-free albedo from Landsat surface reflectance and MODIS BRDF, *Remote Sens. Environ.*, *115*, 2204–2216, doi:10.1016/j.rse.2011.04.019.

Shuai, Y., J. G. Masek, F. Gao, C. B. Schaaf, and T. He (2014), An approach for the long-term 30-m land surface snow-free albedo retrieval from historic Landsat surface reflectance and MODIS-based a priori anisotropy knowledge, *Remote Sens. Environ.*, *152*, 467–479, doi:10.1016/j.rse.2014.07.009.

Steffen, K., and J. Box (2001), Surface climatology of the Greenland ice sheet: Greenland Climate Network 1995-1999, *J. Geophys. Res. Atmos.*, doi:10.1029/2001JD900161.

Stroeve, J., J. E. Box, F. Gao, S. Liang, A. Nolin, and C. Schaaf (2005), Accuracy assessment of the MODIS 16-day albedo product for snow: Comparisons with Greenland in situ measurements, *Remote Sens. Environ.*, *94*, 46–60, doi:10.1016/j.rse.2004.09.001.

Stroeve, J. C., J. E. Box, and T. Haran (2006), Evaluation of the MODIS (MOD10A1) daily snow albedo product over the Greenland ice sheet, *Remote Sens. Environ.*, *105*(2), 155–171, doi:10.1016/j.rse.2006.06.009.

Sütterlin, M., C. B. Schaaf, R. Stöckli, Q. Sun, F. Hüsler, C. Neuhaus, and S. Wunderle (2015), Albedo and reflectance anisotropy retrieval from AVHRR operated onboard NOAA and MetOp satellites: Algorithm performance and accuracy assessment for Europe, *Remote Sens. Environ.*, doi:10.1016/j.rse.2015.06.023.

Taberner, M., B. Pinty, Y. Govaerts, S. Liang, M. M. Verstraete, N. Gobron, and J. L. Widlowski (2010), Comparison of MISR and MODIS land surface albedos: Methodology, *J. Geophys. Res.*, *115*(D0510), doi:doi:10.1029/2009JD012665.

Toller, G., X. Xiong, J. Sun, B. N. Wenny, X. Geng, J. Kuyper, A. Angal, H. Chen, S. Madhavan, and A. Wu (2013), Terra and Aqua moderate-resolution imaging spectroradiometer collection 6 level 1B algorithm, *J. Appl. Remote Sens.*, *7*(1), 073557, doi:10.1117/1.JRS.7.073557.

Wang, D., S. Liang, T. He, and Y. Yu (2013), Direct estimation of land surface albedo from VIIRS data: Algorithm improvement and preliminary validation, *J. Geophys. Res. Atmos.*, *118*(22), 12,577-12,586, doi:10.1002/2013JD020417.

Wang, L., J. N. S. Cole, P. Bartlett, D. Verseghy, C. Derksen, R. Brown, and K. Von Salzen (2016), Investigating the spread in surface albedo for snow-covered forests in CMIP5 models, *J. Geophys. Res.*, doi:10.1002/2015JD023824.

Wang, Z., C. B. Schaaf, M. J. Chopping, A. H. Strahler, J. Wang, M. O. Román, A. V. Rocha, C. E. Woodcock, and Y. Shuai (2012), Evaluation of Moderate-resolution Imaging Spectroradiometer (MODIS) snow albedo product (MCD43A) over tundra, *Remote Sens. Environ.*, *117*, 264–280, doi:10.1016/j.rse.2011.10.002.

Wang, Z., C. B. Schaaf, A. H. Strahler, M. J. Chopping, M. O. Rom??n, Y. Shuai, C. E. Woodcock, D. Y. Hollinger, and D. R. Fitzjarrald (2014), Evaluation of MODIS albedo product (MCD43A) over grassland, agriculture and forest surface types during dormant and snow-covered periods, *Remote Sens. Environ.*, *140*, 60–77, doi:10.1016/j.rse.2013.08.025.

Wang, Z. et al. (2017), Monitoring land surface albedo and vegetation dynamics using high spatial and temporal resolution synthetic time series from Landsat and the MODIS BRDF/NBAR/albedo product, *Int. J. Appl. Earth Obs. Geoinf.*, doi:10.1016/j.jag.2017.03.008.

Wanner, W.; Li, X.; Strahler, A.H. (1995), On the derivation of kernels for kernel-driven models of bidirectional reflectance. *J. Geophys. Res. Atmos.,* 100, 21077–21089

Woodcock, C. E., A. H. Strahler, and D. L. B. Jupp (1988a), The use of variograms in remote sensing: I. Scene models and simulated images, *Remote Sens. Environ.*, doi:10.1016/0034-4257(88)90108-3.

Woodcock, C. E., A. H. Strahler, and D. L. B. Jupp (1988b), The use of variograms in remote sensing: II. Real digital images, *Remote Sens. Environ.*, doi:10.1016/0034-4257(88)90109-5.

Appendix A

Site name	Latitude	Longitude	Land types	Networks
Alert	82.49	-62.42	Tundra	BSRN
Barrow	71.323	-156.607	Tundra	BSRN-SURFRAD
Boulder	40.05	-105.007	Grassland	BSRN
Cabauw	51.9711	4.9267	Grassland	BSRN
Payerne	46.815	6.944	Cultivated	BSRN
Concordia Station, Dome C	-75.1	123.383	Glacier	BSRN
Gobabeb	-23.5614	15.042	Desert	BSRN
Georg von Neumayer	-70.65	-8.25	Iceshelf	BSRN
Izaña	28.3093	-16.4993	Rock	BSRN
Ny-Ålesund	78.925	11.93	Tundra	BSRN
Syowa	-69.005	39.589	Sea ice	BSRN
Tateno	36.0581	140.1258	Grassland	BSRN
Tiksi	71.5862	128.9188	Tundra	BSRN
Toravere	58.254	26.462	Grassland	BSRN
Bondville	40.0667	-88.3667	Grassland	BSRN-SURFRAD
Table Mountain	40.125	-105.237	Grassland	BSRN-SURFRAD
Desert Rock	36.626	-116.018	Desert	BSRN-SURFRAD
Southern Great Plains	36.605	-97.485	Grassland	BSRN-SURFRAD
Darwin	-12.425	130.891	Grassland	BSRN
Fort Peck	48.3167	-105.1	Grassland	BSRN-SURFRAD
Goodwin Creek	34.2547	-89.8729	Grassland	BSRN-SURFRAD
Rock Springs	40.72	-77.9333	Cultivated	BSRN
Sioux Falls	43.73	-96.62	Grassland	BSRN-SURFRAD
Pu'u Maka'ala Natural Area Reserve	19.55309	-155.317	Evergreen Forest	NEON
Onaqui	40.17759	-112.452	Shrub	NEON
Santa Rita Experimental Range	31.91068	-110.835	Shrub	NEON
Niwot Ridge Mountain Research Station	40.05425	-105.582	Grassland	NEON
Yellowstone Northern Range (Frog Rock)	44.95348	-110.539	Sparse Evergreen Forest	NEON

LBJ National Grasslandland	33.40123	-97.57	Deciduous Forest	NEON
Wind River Experimental Forest	45.82049	-121.952	Evergreen Forest	NEON
Caribou-Poker Creeks Research Watershed	65.15401	-147.503	Mixed Forests	NEON
Toolik	68.66109	-149.37	Tundra	NEON
San Joaquin Experimental Range	37.10878	-119.732	Sparse Evergreen Forest	NEON
Central Plains Experimental Range	40.81553	-104.746	Grassland	NEON
UNDERC	46.23388	-89.5373	Mixed Forest	NEON
Guanica Forest	17.96955	-66.8687	Evergreen Forest	NEON
Ordway-Swisher Biological Station	29.68927	-81.9934	Evergreen Forest	NEON
Smithsonian Conservation Biology Institute	38.89292	-78.1395	Deciduous Forest	NEON
Konza Prairie Biological Station	39.10077	-96.5631	Grassland	NEON
Woodworth	47.12823	-99.2414	Grassland	NEON
Talladega National Forest	32.95046	-87.3933	Mixed Forest	NEON
Oak Ridge	35.96412	-84.2826	Deciduous Forest	NEON
Harvard Forest	42.5369	-72.1727	Deciduous Forest	NEON
Swiss Camp	69.5732	-49.2952	Snow/ice	GC-NET
CP1	69.8819	-46.9763	Snow/ice	GC-NET
NASA-U	73.8333	-49.4953	Snow/ice	GC-NET
GITS	77.1433	-69.095	Snow/ice	GC-NET
Humboldt	78.5266	-56.8305	Snow/ice	GC-NET
Summit	72.5794	-38.5042	Snow/ice	GC-NET
Tunu-N	78.0168	-33.9939	Snow/ice	GC-NET
DYE-2	66.481	-46.28	Snow/ice	GC-NET
JAR1	69.4984	-49.6816	Snow/ice	GC-NET
Saddle	66.0006	-44.5014	Snow/ice	GC-NET
South Dome	63.1489	-44.8167	Snow/ice	GC-NET
NASA-E	75	-29.9997	Snow/ice	GC-NET
CP2	69.9133	-46.8547	Snow/ice	GC-NET
NGRIP	75.0998	-42.3326	Snow/ice	GC-NET
NASA-SE	66.4797	-42.5002	Snow/ice	GC-NET
KAR	69.6995	-32.9998	Snow/ice	GC-NET
JAR2	69.42	-50.0575	Snow/ice	GC-NET
KULU	65.7584	-39.6018	Snow/ice	GC-NET
JAR3	69.3954	-50.3104	Snow/ice	GC-NET

Aurora	67.1352	-47.2911	Snow/ice	GC-NET
Petermann Gl.	80.6836	-60.2931	Snow/ice	GC-NET
AT-Neu	47.1167	11.3175	Grasslands	FLUXNET
AU-Ade	-13.0769	131.1178	Woody Savannas	FLUXNET
AU-ASM	-22.283	133.249	Evergreen Needleleaf Forests	FLUXNET
AU-Cpr	-34.0021	140.5891	Savannas	FLUXNET
AU-Cum	-33.6152	150.7236	Evergreen Broadleaf Forests	FLUXNET
AU-DaP	-14.0633	131.3181	Grasslands	FLUXNET
AU-DaS	-14.1593	131.3881	Savannas	FLUXNET
AU-Dry	-15.2588	132.3706	Savannas	FLUXNET
AU-Emr	-23.8587	148.4746	Grasslands	FLUXNET
AU-Fog	-12.5452	131.3072	Permanent Wetlands	FLUXNET
AU-Gin	-31.3764	115.7138	Woody Savannas	FLUXNET
AU-GWW	-30.1913	120.6541	Savannas	FLUXNET
AU-How	-12.4943	131.1523	Woody Savannas	FLUXNET
AU-Lox	-34.4704	140.6551	Deciduous Broadleaf Forests	FLUXNET
AU-RDF	-14.5636	132.4776	Woody Savannas	FLUXNET
AU-Rig	-36.6499	145.5759	Grasslands	FLUXNET
AU-Rob	-17.1175	145.6301	Evergreen Broadleaf Forests	FLUXNET
AU-Stp	-17.1507	133.3502	Grasslands	FLUXNET
AU-TTE	-22.287	133.64	Open Shrublands	FLUXNET
AU-Tum	-35.6566	148.1517	Evergreen Broadleaf Forests	FLUXNET
AU-Wac	-37.4259	145.1878	Evergreen Broadleaf Forests	FLUXNET
AU-Whr	-36.6732	145.0294	Evergreen Broadleaf Forests	FLUXNET
AU-Wom	-37.4222	144.0944	Evergreen Broadleaf Forests	FLUXNET
AU-Ync	-34.9893	146.2907	Grasslands	FLUXNET
BE-Bra	51.3076	4.5198	Mixed Forests	FLUXNET
BE-Lon	50.5516	4.7461	Croplands	FLUXNET
BR-Sa3	-3.018	-54.9714	Evergreen Broadleaf Forests	FLUXNET
CA-Gro	48.2167	-82.1556	Mixed Forests	FLUXNET
CA-NS1	55.8792	-98.4839	Evergreen Needleleaf Forests	FLUXNET
CA-NS2	55.9058	-98.5247	Evergreen Needleleaf Forests	FLUXNET

CA-NS3	55.9117	-98.3822	Evergreen Needleleaf Forests	FLUXNET
CA-NS4	55.9144	-98.3806	Evergreen Needleleaf Forests	FLUXNET
CA-NS5	55.8631	-98.485	Evergreen Needleleaf Forests	FLUXNET
CA-NS6	55.9167	-98.9644	Open Shrublands	FLUXNET
CA-NS7	56.6358	-99.9483	Open Shrublands	FLUXNET
CA-Oas	53.6289	-106.198	Deciduous Broadleaf Forests	FLUXNET
CA-Obs	53.9872	-105.118	Evergreen Needleleaf Forests	FLUXNET
CA-Qfo	49.6925	-74.3421	Evergreen Needleleaf Forests	FLUXNET
CA-SF1	54.485	-105.818	Evergreen Needleleaf Forests	FLUXNET
CA-SF2	54.2539	-105.878	Evergreen Needleleaf Forests	FLUXNET
CA-SF3	54.0916	-106.005	Open Shrublands	FLUXNET
CA-TP4	42.7102	-80.3574	Evergreen Needleleaf Forests	FLUXNET
CA-TPD	42.6353	-80.5577	Deciduous Broadleaf Forests	FLUXNET
CH-Cha	47.2102	8.4104	Grasslands	FLUXNET
CH-Dav	46.8153	9.8559	Evergreen Needleleaf Forests	FLUXNET
CH-Fru	47.1158	8.5378	Grasslands	FLUXNET
CH-Oe1	47.2858	7.7319	Grasslands	FLUXNET
CN-Cng	44.5934	123.5092	Grasslands	FLUXNET
CN-HaM	37.37	101.18	Grasslands	FLUXNET
CZ-BK1	49.5021	18.5369	Evergreen Needleleaf Forests	FLUXNET
CZ-BK2	49.4944	18.5429	Grasslands	FLUXNET
CZ-Permanent Wetlands	49.0247	14.7704	Permanent Wetlands	FLUXNET
DE-Akm	53.8662	13.6834	Permanent Wetlands	FLUXNET
DE-Geb	51.1001	10.9143	Croplands	FLUXNET
DE-Gri	50.95	13.5126	Grasslands	FLUXNET
DE-Hai	51.0792	10.453	Deciduous Broadleaf Forests	FLUXNET
DE-Kli	50.8931	13.5224	Croplands	FLUXNET
DE-Lkb	49.0996	13.3047	Evergreen Needleleaf Forests	FLUXNET
DE-Lnf	51.3282	10.3678	Deciduous Broadleaf Forests	FLUXNET

DE-Obe	50.7867	13.7213	Evergreen Needleleaf Forests	FLUXNET
DE-RuR	50.6219	6.3041	Grasslands	FLUXNET
DE-RuS	50.8659	6.4472	Croplands	FLUXNET
DE-SfN	47.8064	11.3275	Permanent Wetlands	FLUXNET
DE-Spw	51.8923	14.0337	Permanent Wetlands	FLUXNET
DE-Tha	50.9624	13.5652	Evergreen Needleleaf Forests	FLUXNET
DE-Zrk	53.8759	12.889	Permanent Wetlands	FLUXNET
DK-NuF	64.1308	-51.3861	Permanent Wetlands	FLUXNET
DK-Sor	55.4859	11.6446	Deciduous Broadleaf Forests	FLUXNET
DK-ZaF	74.4814	-20.5545	Permanent Wetlands	FLUXNET
DK-ZaH	74.4733	-20.5503	Grasslands	FLUXNET
FI-Hyy	61.8474	24.2948	Evergreen Needleleaf Forests	FLUXNET
FI-Jok	60.8986	23.5135	Croplands	FLUXNET
FI-Let	60.6418	23.9595	Evergreen Needleleaf Forests	FLUXNET
FI-Lom	67.9972	24.2092	Permanent Wetlands	FLUXNET
FR-Gri	48.8442	1.9519	Croplands	FLUXNET
FR-LBr	44.7171	-0.7693	Evergreen Needleleaf Forests	FLUXNET
FR-Pue	43.7413	3.5957	Evergreen Broadleaf Forests	FLUXNET
GF-Guy	5.2788	-52.9249	Evergreen Broadleaf Forests	FLUXNET
GH-Ank	5.2685	-2.6942	Evergreen Broadleaf Forests	FLUXNET
IT-BCi	40.5238	14.9574	Croplands	FLUXNET
IT-CA1	42.3804	12.0266	Deciduous Broadleaf Forests	FLUXNET
IT-CA2	42.3772	12.026	Croplands	FLUXNET
IT-CA3	42.38	12.0222	Deciduous Broadleaf Forests	FLUXNET
IT-Col	41.8494	13.5881	Deciduous Broadleaf Forests	FLUXNET
IT-Isp	45.8126	8.6336	Deciduous Broadleaf Forests	FLUXNET
IT-La2	45.9542	11.2853	Evergreen Needleleaf Forests	FLUXNET
IT-Lav	45.9562	11.2813	Evergreen Needleleaf Forests	FLUXNET
IT-MBo	46.0147	11.0458	Grasslands	FLUXNET
IT-Noe	40.6062	8.1512	Closed Shrublands	FLUXNET

IT-Ren	46.5869	11.4337	Evergreen Needleleaf Forests	FLUXNET
IT-Ro1	42.4081	11.93	Deciduous Broadleaf Forests	FLUXNET
IT-Ro2	42.3903	11.9209	Deciduous Broadleaf Forests	FLUXNET
IT-SR2	43.732	10.291	Evergreen Needleleaf Forests	FLUXNET
IT-SRo	43.7279	10.2844	Evergreen Needleleaf Forests	FLUXNET
IT-Tor	45.8444	7.5781	Grasslands	FLUXNET
JP-MBF	44.3869	142.3186	Deciduous Broadleaf Forests	FLUXNET
JP-SMixed Forests	35.2617	137.0788	Mixed Forests	FLUXNET
MY-PSO	2.973	102.3062	Evergreen Broadleaf Forests	FLUXNET
NL-Hor	52.2404	5.0713	Grasslands	FLUXNET
NO-Adv	78.186	15.923	Permanent Wetlands	FLUXNET
NO-blv	78.186	15.923	Permanent Wetlands	FLUXNET
RU-Che	68.613	161.3414	Permanent Wetlands	FLUXNET
RU-Fyo	56.4615	32.9221	Evergreen Needleleaf Forests	FLUXNET
RU-Sam	72.3738	126.4958	Grasslands	FLUXNET
RU-Tks	71.5943	128.8878	Grasslands	FLUXNET
SE-Stl	68.3542	19.0503	Permanent Wetlands	FLUXNET
SN-Dhr	15.4028	-15.4322	Savannas	FLUXNET
US-ARL	36.4267	-99.42	Grasslands	FLUXNET
US-AR2	36.6358	-99.5975	Grasslands	FLUXNET
US-ARM	36.6058	-97.4888	Croplands	FLUXNET
US-Cop	38.09	-109.39	Grasslands	FLUXNET
US-CRT	41.6285	-83.3471	Croplands	FLUXNET
US-GBT	41.3658	-106.24	Evergreen Needleleaf Forests	FLUXNET
US-GLE	41.3665	-106.24	Evergreen Needleleaf Forests	FLUXNET
US-GOO	34.2547	-89.8735	Grasslands	FLUXNET
US-IB2	41.8406	-88.241	Grasslands	FLUXNET
US-Ivo	68.4865	-155.75	Permanent Wetlands	FLUXNET
US-Los	46.0827	-89.9792	Permanent Wetlands	FLUXNET
US-Me2	44.4523	-121.557	Evergreen Needleleaf Forests	FLUXNET
US-Me3	44.3154	-121.608	Evergreen Needleleaf Forests	FLUXNET
US-Me6	44.3233	-121.608	Evergreen Needleleaf Forests	FLUXNET

US-MMS	39.3232	-86.4131	Deciduous Broadleaf Forests	FLUXNET
US-Ne1	41.1651	-96.4766	Croplands	FLUXNET
US-Ne2	41.1649	-96.4701	Croplands	FLUXNET
US-Ne3	41.1797	-96.4397	Croplands	FLUXNET
US-NR1	40.0329	-105.546	Evergreen Needleleaf Forests	FLUXNET
US-Oho	41.5545	-83.8438	Deciduous Broadleaf Forests	FLUXNET
US-ORv	40.0201	-83.0183	Permanent Wetlands	FLUXNET
US-Prr	65.1237	-147.488	Evergreen Needleleaf Forests	FLUXNET
US-SRC	31.9083	-110.84	Open Shrublands	FLUXNET
US-SRG	31.7894	-110.828	Grasslands	FLUXNET
US-SRM	31.8214	-110.866	Woody Savannas	FLUXNET
US-Syv	46.242	-89.3477	Mixed Forests	FLUXNET
US-Tw1	38.1074	-121.647	Permanent Wetlands	FLUXNET
US-Tw2	38.1047	-121.643	Croplands	FLUXNET
US-Tw3	38.1159	-121.647	Croplands	FLUXNET
US-Tw4	38.103	-121.641	Permanent Wetlands	FLUXNET
US-UMB	45.5598	-84.7138	Deciduous Broadleaf Forests	FLUXNET
US-UMd	45.5625	-84.6975	Deciduous Broadleaf Forests	FLUXNET
US-Var	38.4133	-120.951	Grasslands	FLUXNET
US-WCr	45.8059	-90.0799	Deciduous Broadleaf Forests	FLUXNET
US-Whs	31.7438	-110.052	Open Shrublands	FLUXNET
US-Wkg	31.7365	-109.942	Grasslands	FLUXNET
US-WPT	41.4646	-82.9962	Permanent Wetlands	FLUXNET
ZA-Kru	-25.0197	31.4969	Savannas	FLUXNET
ZM-Mon	-15.4378	23.2528	Deciduous Broadleaf Forests	FLUXNET
KPC_L	79.9108	-24.0828	Snow/ice	PROMICE
KPC_U	79.8347	-25.1662	Snow/ice	PROMICE
EGP	75.6247	-35.9748	Snow/ice	PROMICE
SCO_L	72.223	-26.8182	Snow/ice	PROMICE
SCO_U	72.3933	-27.2333	Snow/ice	PROMICE
MIT	65.6922	-37.828	Snow/ice	PROMICE
TAS_L	65.6402	-38.8987	Snow/ice	PROMICE
TAS_U	65.6978	-38.8668	Snow/ice	PROMICE
TAS_A	65.779	-38.8995	Snow/ice	PROMICE
QAS_L	61.0308	-46.8493	Snow/ice	PROMICE
QAS_M	61.0998	-46.833	Snow/ice	PROMICE

QAS_U	61.1753	-46.8195	Snow/ice	PROMICE
QAS_A	61.243	-46.7328	Snow/ice	PROMICE
NUK_L	64.4822	-49.5358	Snow/ice	PROMICE
NUK_U	64.5108	-49.2692	Snow/ice	PROMICE
NUK_K	64.1623	-51.3587	Snow/ice	PROMICE
NUK_N	64.9452	-49.885	Snow/ice	PROMICE
KAN_B	67.1252	-50.1832	Snow/ice	PROMICE
KAN_L	67.0955	-49.9513	Snow/ice	PROMICE
KAN_M	67.067	-48.8355	Snow/ice	PROMICE
KAN_U	67.0003	-47.0253	Snow/ice	PROMICE
UPE_L	72.8932	-54.2955	Snow/ice	PROMICE
UPE_U	72.8878	-53.5783	Snow/ice	PROMICE
THU_L	76.3998	-68.2665	Snow/ice	PROMICE
THU_U	76.4197	-68.1463	Snow/ice	PROMICE